



Reservoir Geology and Basin Analysis Group

Department of Earth Sciences
University of Geneva



3D static models of the GEO-01 and GEO-02 exploration wells

Report n.	GEG2021007
Date	12.10.2018
Author (s)	Ovie Eruteya Luca Guglielmetti Andrea Moscariello
Approved by	Luca Guglielmetti, Andrea Moscariello



Table of contents

1. SUMMARY	3
2. INTRODUCTION	5
3. GEOLOGIC SETTING	6
4. Dataset and Methods	8
4.1. Dataset	9
5. Methodological Workflow	11
5.1. Seismic Interpretation.....	11
5.2. Well log interpretation.....	11
6. 3-D subsurface geological model and static model development	11
7. Results and Interpretations	12
7.1. Seismic Stratigraphy of the main units of interest and lithological description.....	12
7.2. Well Correlation between GGeo-01 and GGeo-02	13
7.3. Seismic Interpretation.....	13
7.4. 3-D Geological Model Development.....	17
7.5. 3D static Modelling for the Cretaceous and Jurassic Reservoirs Across GGeo-01 and GGeo-02.	20
8. Discussions	22
8.1. Uncertainties associated with the 3-D Geological Model development around the GGeo-01 and GGeo-02 area.....	22
8.2. Impact of 3-D geological model, Petrophysical and facies properties on geothermal reservoir – Lower Cretaceous Unit.....	24
8.3. Implication of hydrocarbon occurrence in the study area on geothermal development.....	25
9. Conceptual model evaluating the storage potential of the study area	26
10. Conclusions	27
REFERENCES	29

Abbreviations

AOI: Area of Interest

VOI: Volume of interest

UNIGE: University of Geneva

TH: Thermo-Hydraulic

THE: Thermo-Hydraulic-Economic

1. SUMMARY

In the framework of the GEOTHERMICA ERA-NET co-funded project-HEASTORE, one of the main challenges related to assessing the technical feasibility and sustainability of High Temperature (~25°C to ~90°C) Aquifer Thermal Energy Storage (HTATES) is subsurface characterization. In this final report we present detailed subsurface characterization of two potential storage sites around the recently drilled GGeo-01 and GGeo-02 geothermal exploration borehole sites situated in the Geneva Basin, Canton of Geneva.

These activities have been carried out in the framework of **Task 1.1 Specification and characterization for ATEs concepts** of the proposal submitted to BFE and **Task 5.3: Model validation for Subsurface dynamics** of the European proposal.

The workflow that was implemented was based on the integration of geophysical and petrophysical data initially available at the beginning of the project and subsequent update of the models as new data become available. The overall approach was based on the baseline that 3D static models serve as inputs in integration with energy system information, to produce dynamic models (thermo-hydraulic TH, Thermo-hydraulic-mechanic THM or HM, thermo-hydraulic-chemical THC and Thermo-hydraulic-economic THE) to predict the performance of HT-ATES systems in Geneva.

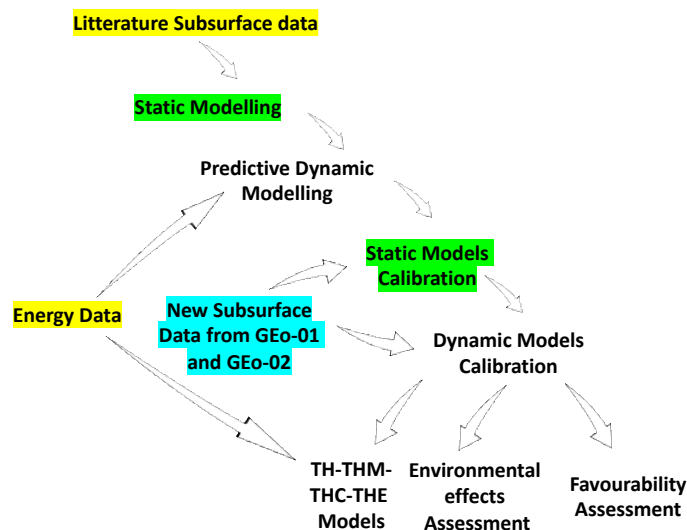


Figure 1 General workflow implemented in HEATSTORE for HT-ATES potential assessment. Highlighted are the different phases involved in the static modelling activities

The results have been achieved from the interpretation of several vintages of 2D seismic reflection dataset, well logs from GGeo-01 and GGeo-02, well reports and outcrop analogues. Seismic interpretation reveals a well-developed flower structure deforming the Mesozoic and parts of the Cenozoic sediments in the GGeo-01 area across all the models developed for this area. On the contrary, the subsurface structural situation around GGeo-02 site is different comprising of thrust faults system and other normal faults deforming the Cenozoic and Mesozoic sediments. Petrophysical analysis suggests the Lower Cretaceous Formation in the GGeo-01 area is tight, generally characterized by low porosity and permeability values. However, the presence of fracture networks and faults deforming a substantial part of this unit may promote localized fluid circulation. Three candidate horizons have been identified as potential Lower Cretaceous targets (CT) suitable for HT-ATES in fractured intervals characterized by

tested water outflows and devoid of hydrocarbon impregnation: (1) Grand Essert Fm / Pierre Jeune de Neuchatel + Marnes d’Hauterives Fm [CT1], (2) Vuache Fm - Chambotte- Chambotte inférieure [CT2] and (3) Goldberg Fm [CT3]. The 3-D static model developed in this study was used as input for numerical heat flow and predictive TH and THE models for the Geneva Basin. In the GEO-02, well test results suggest that the formations within the Mesozoic succession have low fluid flow and weak hydraulic properties. The multi-scenario modelling adopted in this study will permit using the different the 3-D geological models developed for GEO-01 and GEO-02 (Figure 1) area as input for further numerical dynamic models to predict the potential of storage in the two areas.

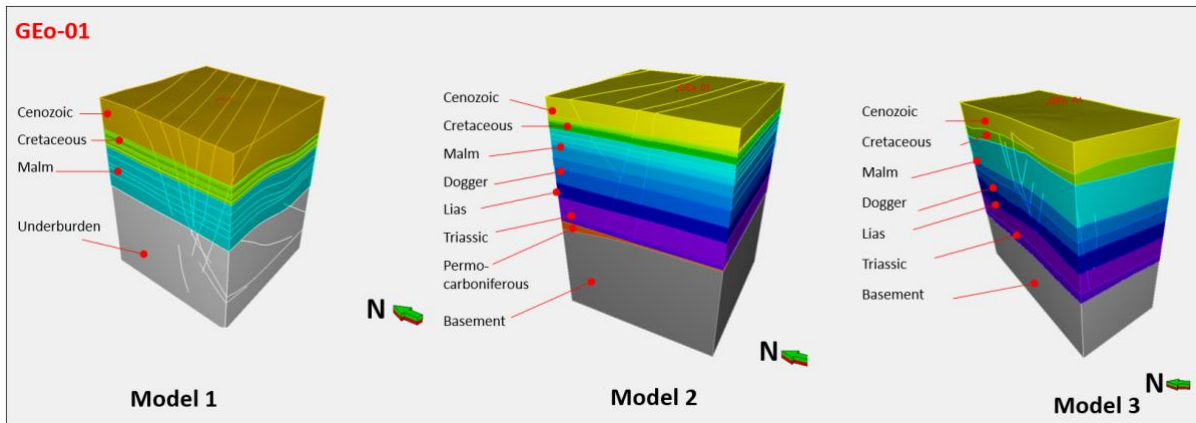


Figure 2 Geological model for the three different structural and stratigraphic frameworks modelled or GEO-01.

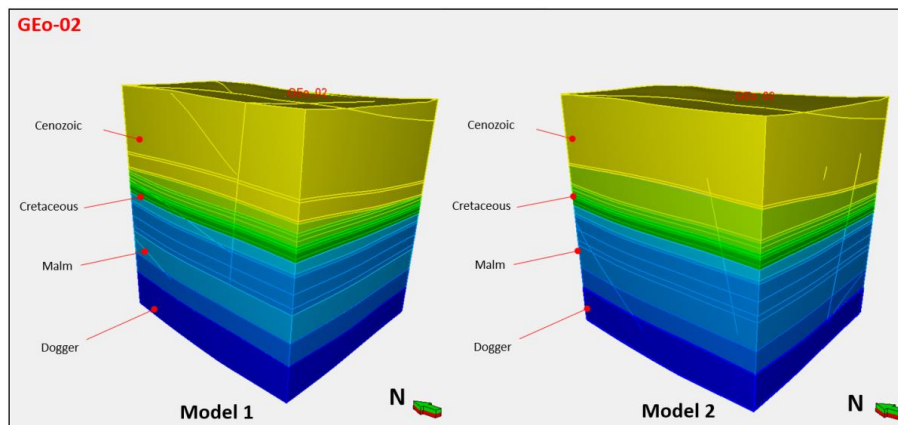


Figure 3 Two different geological model (Model-1 and Model-2) developed for GEO 2 arising from the two different structural model used as input.

The results of these project provided a detailed evolution of the knowledge of the subsurface geology in this segment of the Swiss Molasse basin is well captured by comparing geological models developed using the pre-drill database developed and post-drill database. Importantly the discovery of 100s of meter thick Siderolithic sediments in GEO-02, not encountered by the GEO-02 suggests the geology of the Geneva Basin, changes dramatically within a short spatial extent impacting the potential of identifying suitable storage reservoirs. In all, our findings highlight the need for subsurface data augmentation in the Geneva Basin. It also shed light on the implication of the subsurface manifestation of hydrocarbons as geohazard to heat storage and other geo-energy related projects at large across the Swiss Molasse Basin.

2. INTRODUCTION

The deployment of renewable energy sources for both power and heat production is accelerating in Europe, a trend that will continue. However, the variations in both the availability and demand for energy and their integration into the existing energy infrastructure raise challenges in terms of operational variability and balancing. Peak shaving and heat storage can help to balance demand and supply to make better use of infrastructure and assets. Thermal energy storage can, for example, be implemented in heating networks in the form of Aquifer Thermal Energy Storage (ATES) to support the use of surplus heat from industry and the implementation of renewable heat sources. ATES involves the temporal storage of sensible heat and cold in the subsurface through the injection and withdrawal of groundwater (Dickson et al. 2009). Furthermore, ATES system may be employed as an auxiliary energy back-up system for storing surplus energy for later utilization usually during periods of peak demand (Bloemendal et al., 2014; McCartney et al., 2016). ATES has been gaining widespread attention based on its low carbon footprint and low thermal emissions when compared to other energy systems. This invariably results in a reduction of the overdependence on other conventional heating and cooling sources thereby reducing cost and the emission of climate-forcing gases which have an implication on global warming. The successful development of an efficient ATES system is challenging as any geo-energy project where understanding and 3D modelling of the subsurface is of primary importance (Moscariello, 2016). Specifically, an ATES project requires detailed subsurface characterization of the proposed storage site, modelling and simulation of different storage scenarios to meet the envisage energy demand. This is critical for a comprehensive understanding of the geothermal plume behaviour over a given storage episode. Moreover, a geologically realistic model is necessary to predict the interaction of subsurface elements, especially the structural framework (faults system) and even geobodies such as channels system with the thermal plume. Some of these elements may adversely promote early thermal breakthrough and may contribute towards thermal pollution of subsurface potable water, and in the extreme possible discharge of groundwater into surface water bodies (Possemiers et al., 2015). Most ATES models are typically built using simplistic grids that do not represent the true geological complexity of the subsurface at the storage site. The uncertainties in subsurface are mostly attributed to the paucity or unavailability of the dense network of subsurface geophysical datasets upon which the model is to be developed. This study is being carried out under the framework of the GEOTHERMICA ERA-NET co-funded project-HEASTORE project and focuses on the development of a static geothermal model for the development of HT-ATES system in Geneva Basin situated in the Western Swiss Plateau (Figure 4).

Two recently drilled geothermal exploration borehole G_{Eo}-01 and G_{Eo}-02 by SIG (Services Industriels de Genève) in the framework of the Geothermie2020 program, targeting fault zones in the Lower Cretaceous carbonates (G_{Eo}-01 area) and Upper Jurassic Carbonates (Malm) (G_{Eo}-02 Area) in the Geneva Basin provides new datasets to assess the potential for geothermal applications including high-temperature ATES. Therefore, the objectives of this projects are to; (1) develop a structural and stratigraphic framework for the study area (2) construct a robust geological model (3) identify potential candidate(s) horizons in G_{Eo}-01 and G_{Eo}-02 area for ATES. This was achieved based on the integration of pre-existing and newly acquired geological, geophysical and petrophysical dataset encompassing seismic reflection datasets, borehole logs and cuttings, and sedimentological dataset from the drilling reports. The multiple models developed across both sites represent a critical input and backbone for future fracture network modelling, numerical thermo-mechanical and geochemical modelling of the ATES system and subsurface fluid flow dynamics within this segment of the Geneva Basin.

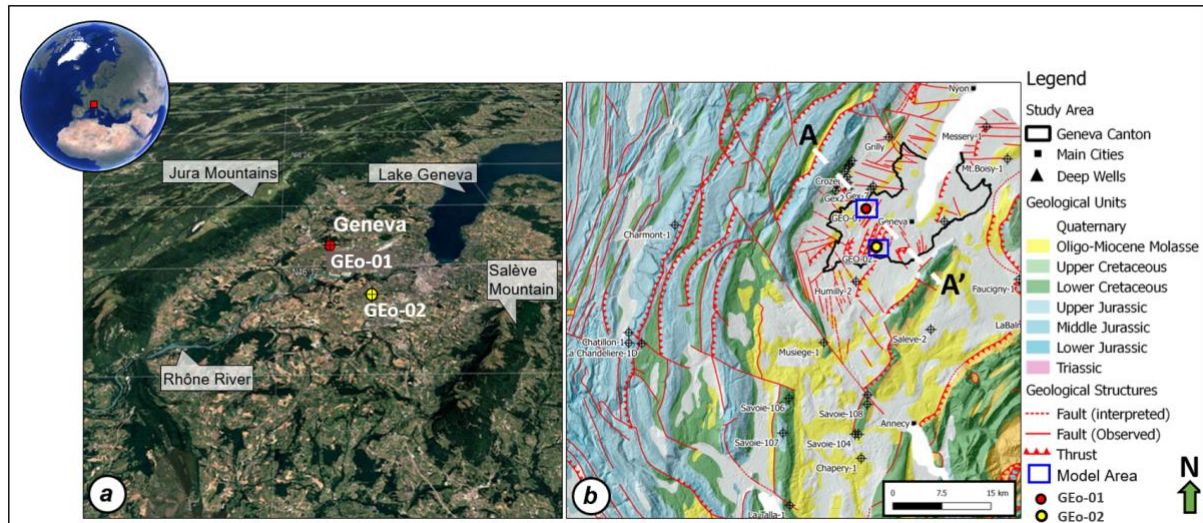


Figure 4 (a) Location of the study area in the Geneva Basin, Switzerland, showing the locations of GEO-01 and GEO-02 (b) The structural situation of the Geneva Basin indicating the fault systems (modified from Moscariello et al., 2020).

3. GEOLOGIC SETTING

The study area is in the Geneva Basin (hereafter GB) in the south-westernmost portion of the Swiss Molasse Basin (Figure 4). The GB is limited to the NW by the Jura Mountains and to the SE by the Salève Mountain. Importantly, the Jura Mountain has been identified as a source for recharging the subsurface aquifers systems in the GB (Murault, 2000, Figure 5). The configuration of the GB is typified by a 2000-3000 m-thick Mesozoic and Cenozoic succession overlaying a Palaeozoic crystalline basement that evolved during the Variscan orogeny (Figure 5). Subsequent to this orogenic episode an extensive rift system developed in the GB resulting in the evolution of a series of SW-NE trending half-graben structures infilled by Permo-Carboniferous sediments - mainly fluvial to lacustrine deposits with some intercalation of coal seams (Gorin et al., 1993, Signer and Gorin 1995; Clerc et al., 2015; Moscariello et al., 2019).

The structural and stratigraphic evolution of the Mesozoic and Cenozoic unit in the GB is modulated by the underlying SW-NE trending half-graben structures and NNW-SSE basement related lineaments (Figure 5 and Figure 6). The NNW-SSE trending lineaments are strike-slip fault zones - Vuache, Cruseilles, Le Coin and Arve fault zones. On a seismic reflection profile, these faults are expressed as wrench faults (Signer and Gorin, 1995). Importantly, these fault zones have been active since the Permo-Carboniferous to recent (Signer and Gorin, 1995). Ongoing hydrothermal exploration activities in the Geneva Basin target these fault zones.

Lower Jurassic deposits show marly carbonates and shales while the Middle Jurassic, alternating bioclastic carbonates and muddier facies testify to a transitional, shallower environment in the carbonate ramp when compared to the underlying unit. The Upper Jurassic unit shows an overall regressive trend, ending at the beginning of the Cretaceous. From the Middle Kimmeridgian until the Lower Tithonian, a coral-microbial patch reef system developed on a large, shallow carbonate platform. The strong diagenetic imprint and numerous fractures evidence a high heterogeneity within this unit but also promising reservoir properties (Makhloufi et al., 2018).

The Cretaceous unit is the focus of this study and has been substantially eroded resulting in the absence of the Upper Cretaceous. The Lower Cretaceous series was deposited in a shallow and warm water

environment characterized by a low amplitude sea-level fluctuation resulting in several episodes of emersion-drowning of the carbonate platform. This resulted in the deposition of a stacked system of alternating limestone and marly limestone layers characterized by tight and shallow carbonate facies. Importantly, this unit displays excellent aquifer/reservoir properties characterized by the localization of abundant fracture networks and karst system (karstification been prominent in the Urgonian limestones) arising from the erosion of this unit. Uplift of the basement arising from the convergence between the Eurasian and African plates resulted in the exhumation of the Mesozoic succession (Trumpy, 1980; Karner and Watts, 1983). The ensuing sub-equatorial climate during this time promoted erosion of the top Cretaceous unit resulting in the development of a major unconformity. Fractures and karst features are common occurrences atop the Mesozoic series and are filled by some reworked Aptian-Albian sediments and some lateritic deposits (Hooker and Weidmann, 2007; Becker et al., 2013).

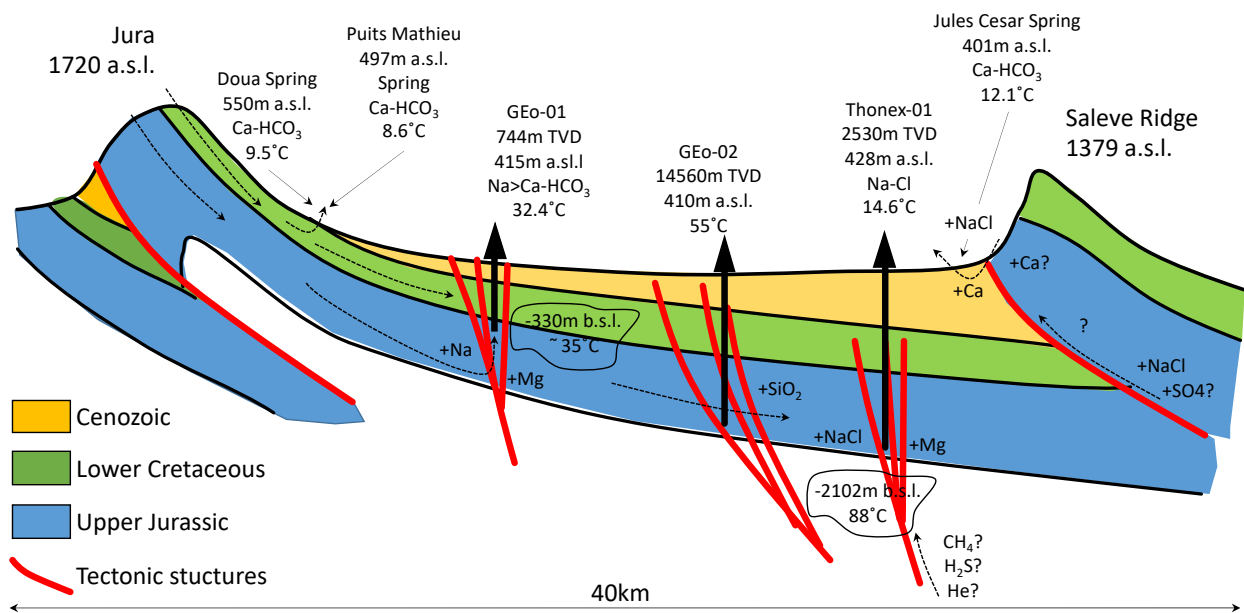


Figure 5 Conceptual model of groundwater circulation in the Geneva Basin modified from Guglielmetti et al. 2020 (vertical and horizontal scales are not proportional).

The Oligocene Lower Freshwater Molasse (USM) is composed of alternated sandstone and marlstone. This unit onlaps the Early Cretaceous unit or the lateritic Eocene sediments. Importantly, the Upper Marine Molasse (OMM) and the Upper Freshwater Molasse (OSM) are missing in the GB due to erosion during glacial advancement (Signer and Gorin, 1995; Charollais et al., 2007) (Figure 6). The topmost unit of the GB consists of Quaternary to recent sediments overlying the Molasse deposits. During the Quaternary several episodes of glaciation prevailed in the GB as recorded by the presence of glaciogenic sediments and tunnel valley systems incising the uppermost Molasse unit arising from the advance and retreat of the Rhone Glacier and its related glaciers (Moscariello, 1996; Moscariello et al., 1998; Fiore et al., 2011). During the Glacial maximum, about 1000 km of ice (Rhone and Arve Glaciers) covered the GB.

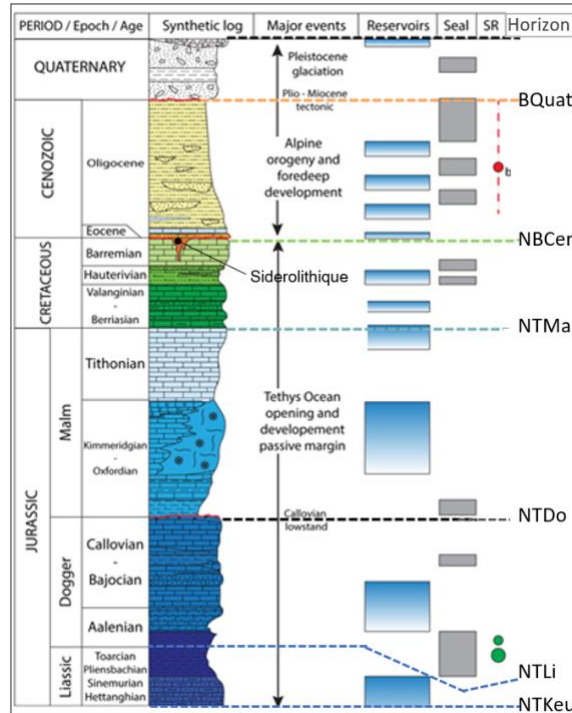


Figure 6 Lithostratigraphy of the Geneva Basin (modified from Moscariello, 2019; Moscariello et al., 2020). Key seismic horizons mapped in this study are indicated here and the formation depth of the Geo-01 well.

4. Dataset and Methods

In order to develop geologically realistic 3D subsurface models, we analysed a suite of subsurface dataset consisting of seismic reflection dataset, borehole, sedimentological information from drilling report and a regional subsurface model- GEOMOL project (Figure 7).

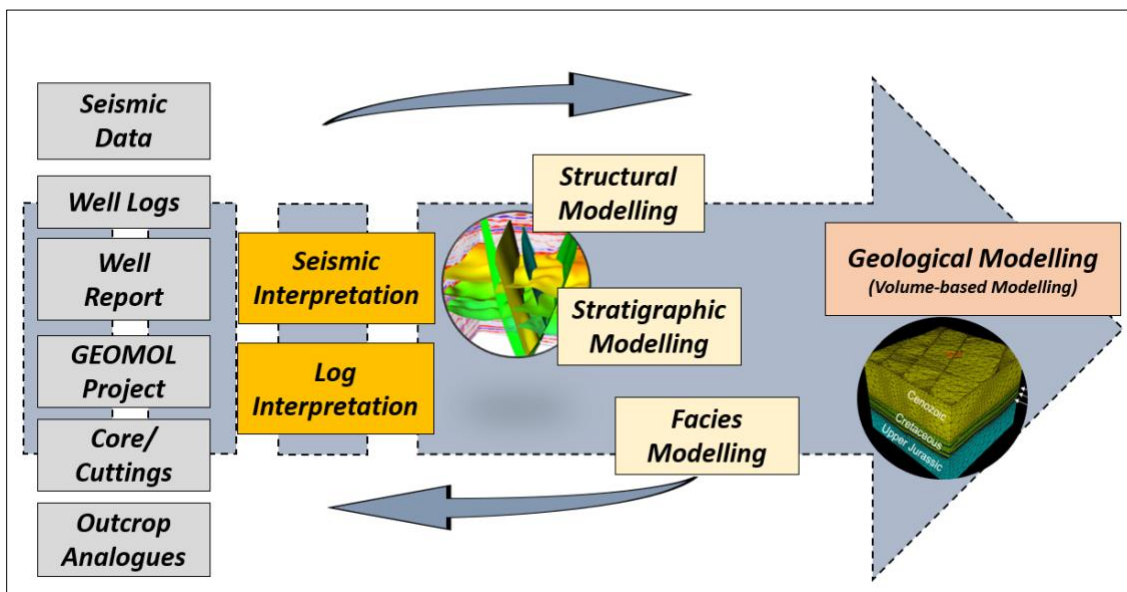


Figure 7 Workflow adopted in this study in developing the subsurface geological models for GGeo-1 and GGeo-02 areas.

4.1. Dataset

4.1.1. 2-D Seismic Reflection Data at GEO-01 site

a. Pre-existing 2D seismic reflection data sets

In the GEO-01 area two 2D seismic reflection surveys are available: 15SIG_08 and GG87_02 (Figure 8). These lines are time-migrated and zero phased). In all, the seismic reflection surveys are time-migrated and zero-phased where a positive polarity for example transition from the Molasse (siliciclastic) to the Lower Cretaceous is represented by a hard kick and appears as a peak in the seismic data.

b. New/reprocessed 2D seismic reflection dataset

An additional 2-D seismic reflection line GECOS-UNIGE-2020 was available in 2020. This line was acquired under the framework of the Innosuisse GECOS project by the University of Geneva in order to reduce uncertainties associated with the faults (Figure 8).

4.1.2. Borehole Dataset - GEO-01 Geothermal Exploration Borehole

The principal borehole analysed in this study is the GEO-01 borehole drilled by SIG (Services Industriels de Genève) in 2018 for geothermal exploration in the Geneva Basin. The GEO-01 borehole was drilled to a measured depth of 744 m, with cuttings recovered for the entire interval, however, only the first 533 m was logged. Borehole logs available from GEO-01 include gamma-ray, spontaneous potential, sonic, caliper, resistivity, density, and neutron. Detailed well report identifying faulted and faulted intervals, hydrocarbon impregnated intervals and key formation tops.

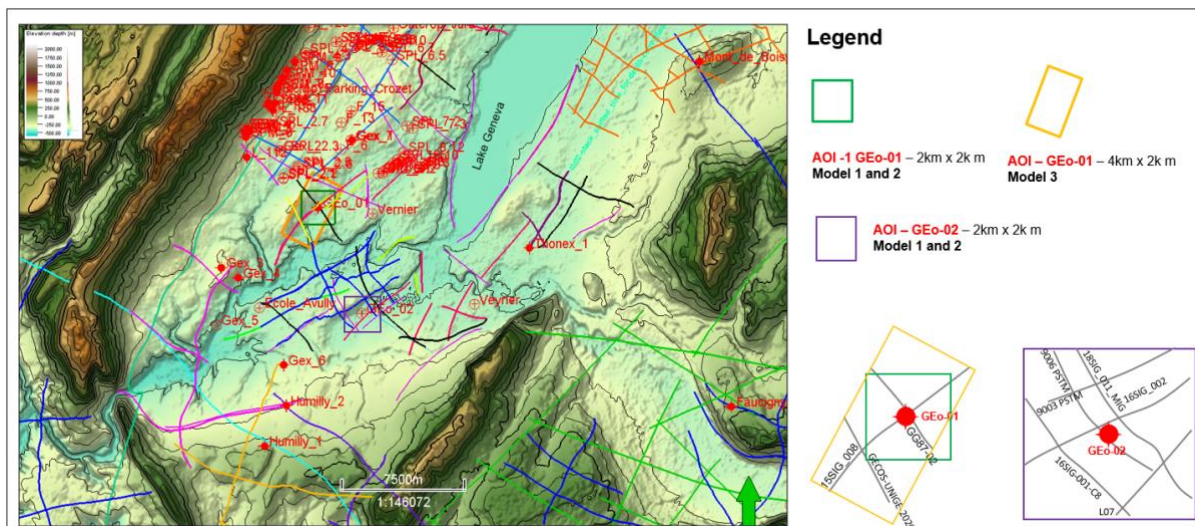


Figure 8 Database available showing 2D seismic reflection survey and boreholes. Area of interest of the various geological models developed for GEO-1 and GEO-02 are indicated.

4.1.3. 2-D Seismic Reflection Data at GGeo-02 site

a. Pre-existing 2D seismic reflection data sets

The initially available line within the Region of interest for developing the subsurface geological model consists of (1) 9006 (2) 16 SIG_001 (3) 18 SIG_011 (4) 18 SIG_009 (5) 18 SIG_012 (6) 18 SIG_010 (7) GG87-04 (8) 16 SIG 01 (9) 14SIG-101 (10) 9002_SIG (10) 18SIG_011.

b. New/reprocessed 2D seismic reflection dataset

In 2021, SIG provided UNIGE of Geneva, newly acquired/reprocessed higher resolution time-migrated 2D seismic reflection dataset around the target area in Bernex. These lines encompass the

- 2020_09_23_SIG_STJULIEN2D_16SIG01_Final_Pre-Migration_Stack;
- 2020_09_23_SIG_STJULIEN2D_16SIG01_Final_Pre-STM;
- 2020_09_23_SIG_STJULIEN2D_18SIG11_Final_Pre-Migration_Stack
- 2020_09_23_SIG_STJULIEN2D_18SIG11_Final_Pre-STM.

4.1.4. Borehole Data- GGeo-02 Geothermal Exploration Borehole

The GGeo-02 borehole was drilled in 2020 by SIG for geothermal exploration purposes in Lully, Bernex in Geneva cartoon (Figure 5). GGeo-02 borehole reached a measured depth of 1455.7 m below the ground level in the Upper Jurassic (Kimmeridgian-Oxfordian). The suite of well logs available from GGeo-02 includes Gamma Ray (Potassium, Uranium and Thorium), Density, Spontaneous Potential, Caliper, Sonic and resistivity logs.

Formation tops for the entire drilled intervals were available from well reports provided by SIG. Also included in these well reports are information concerning potential aquifers and presence of hydrocarbon occurrences, which are of implication to subsurface heat storage.

4.1.5. Pre-existing regional Subsurface Model - GEOMOL Project

GEOMOL project is a 3-D geological model of the Swiss Plateau created from the analysis of a large dataset of 2-D and now recently 3-D seismic reflection surveys, shallow and deep boreholes, geological sections and topographic maps. (<https://www.swisstopo.admin.ch/en/knowledge-facts/geology/geological-data/3d-geology/deep/geomol.html>). The GEOMOL project consists of key geological surfaces and faults In the course of this project we have extracted key stratigraphic surfaces within our volume of interest from the GEOMOL v 2016 project and GEOMOL v 2019 (available online at <https://ge.ch/sitg/>) as starting points for subsurface interpretation. Importantly, the velocity model from GEOMOLv2016 was employed for time-depth conversion.

4.1.6. Digital Elevation

The Aster digital elevation model was used to reveal the geomorphology of the ground level across the GGeo-01 and GGeo-02 Areas (available online at <https://asterweb.jpl.nasa.gov/gdem.asp>). The Aster digital elevation model has a resolution of 30 m.

5. Methodological Workflow

5.1. Seismic Interpretation

All interpretations and modelling were performed using Schlumberger's Petrel (version 2018 and 2020) seismic interpretation software available at the Geo--Energy/ Reservoir geology and Basin analysis group and guided by the previously existing tectonostratigraphic framework of the Geneva Basin (e.g. Clerc et al., 2015). A classical seismic interpretation technique was performed involving mapping key stratigraphic horizons of interest, paying attention to key faults were mapped as vertical to sub-vertical zones of discontinuity in the seismic reflectors in the seismic dataset. Since we analysed 2-D seismic profiles, fault planes were established by connecting the most likely faults intersections on the seismic profile. In order instances where this could not be achieved due to non-intersecting seismic lines, we opted for a knowledge-driven interpretation by extending the fault plane along a preferred direction based on the geological context and literature (e.g. Clerc et al., 2015; Moscariello et al., 2020). The fault networks and key horizons were converted from time to depth on the fly using the velocity model in the GEOMOL project to generate a structural model for the study area (Figure 4). In the case of GGeo-02 we used the checkshot data available for time to depth conversion of the interpreted faults and horizons. However, during the quality control process, minor adjustments were made to the interpretations based on the formation tops available from the newly drilled GGeo-01 and GGeo-02 boreholes.

A multi-scenario seismic interpretation was performed to capture the subsurface complexity around the GGeo-01 and GGeo-02 area. This was also necessary as reprocessed and new seismic reflection dataset became available during the life cycle of the project. Therefore, different geologically plausible subsurface structural and stratigraphic interpretations were presented. These multiple scenarios were then used as input in developing multiple 3D subsurface models around the GGeo-01 and GGeo-02 area.

5.2. Well log interpretation

Well logs and formation top available from the GGeo-01 and GGeo-02 borehole were imported into Petrel v 2018 and 2020. This will permit integration with the seismic reflection dataset available. The well logs were quality controlled for bad data points prior to interpretation. Lithological and petrophysical analysis were performed for the wells. Intervals with subsurface manifestation of hydrocarbons were also identified. Candidate intervals for the heat storage were identified as regions with good flow rate, petrophysical properties, bounded above and below by tight formation and devoid of any hydrocarbon manifestation. The latter is to prevent enhanced oil recovery in case of heat injection into such hydrocarbon prone formations

6. 3-D subsurface geological model and static model development

A volume-based modelling approach embedded in Petrel was employed in constructing different subsurface geological models (Figure 9). The earlier structural and stratigraphic interpretations generated from the seismic interpretation workflow were inputted in a predefined Area of interest (AOI) for the GGeo-01 area spanning 2 km x 2 km (GGeo-01 Model 1 and GGeo-01 Model 2) and GGeo-01 Model 3 which incorporates interpretation from the newly acquired GECOS-UNIGE 2D spanning 4 km x 2 km (Figure 8). Also, for the GGeo-02 Area an AOI of 2 km x 2 km model was adopted for GGeo-02- Model 1 and GGeo-02-Model 2 (Figure 8).

Subsequently, fault framework and layering, zonation and structural gridding were performed. Property modelling involving facies modelling and petrophysical modelling was performed based on the

assumption that lithofacies are homogenous and petrophysical properties are homogenous laterally. However, this will vary temporally at the scale of the different formations or aquifers encountered by the GGeo-01 and GGeo-02 borehole. This approach is reasonable based on the availability of only one borehole within AOI at the GGeo-01 and GGeo-02 area. Therefore, further geostatistical modelling may lead to erroneous model development. Porosity and permeability values were difficult to derive from the borehole log in the Geo-01 since the entire interval was not logged. Furthermore, calliper logs reveal the deterioration of borehole conditions which indeed will lead to spurious log-derived petrophysical estimates. To remedy this, we relied on petrophysical measurement from wells elsewhere in the Geneva Basin penetrating the similar formation. This measurement has been derived from core plugs from the Gex borehole and Humily-2 borehole (Rusillon and Chablais, 2017). By late 2020, a new well-test dataset provided a more reliable porosity and permeability dataset. For the GGeo-02 well we used a petrophysical dataset available from the well report for the property modelling. The grid was then populated with this petrophysical property per storage interval and non-storage interval.

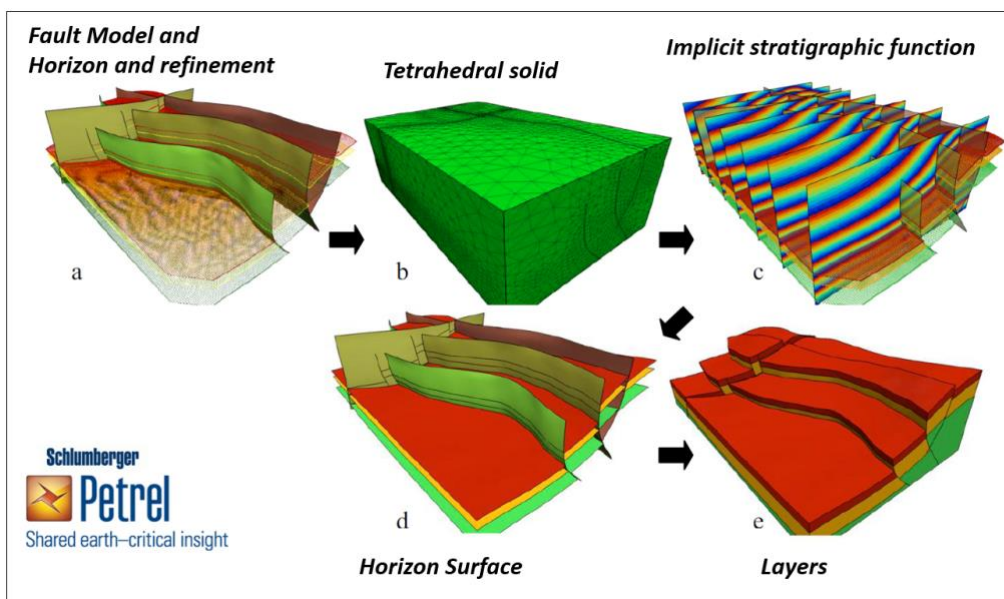


Figure 9 Workflow adopted for development of geological models for GGeo-01 and GGeo-02 areas using the volume-based modelling approach.

7. Results and Interpretations

7.1. Seismic Stratigraphy of the main units of interest and lithological description

Although we have interpreted the seismic dataset up to the basement in some instances, the main unit of interest in this study are the Upper Jurassic (Malm), Lower Cretaceous and the Cenozoic (Molasse). The study area was divided into three major seismic units (SU) based on variation in amplitude and frequency of the seismic reflectors reflecting changes in lithology and density of the subsurface formation (Figure 10-Figure 15).

Upper Jurassic Unit (SU-1): This unit is the basement for the interval of interest in this study. The upper part consists of continuous high amplitude reflections while the lower unit consists of low amplitude semi-transparent to chaotic facies reflections. This unit is bounded at the top by the Near Top Upper Malm horizon. The lithology consisting of this unit is characterized by limestone and dolomite intervals

as penetrated by the GEO-01 and GEO-02 borehole (Figure 9).

Lower Cretaceous Unit (SU-2): The Lower Cretaceous is the unit of interest for the ATES. This unit is bounded by the Base Cenozoic Horizon and Near Top Upper Malm horizon. The reflectors are continuous high amplitude to semi-continuous reflectors in areas affected by deformation related to faulting. Thickness appears to be uniform. The GEO-01 and GEO-02 well reveals this unit is predominantly carbonate dominated, consisting of massive limestones unit with occasionally marly intervals (Figure 9).

Cenozoic Unit (SU-3): The Molasse unit is bounded by the Ground level and Base Cenozoic Horizon. The Molasse sediments onlaps the underlying Cretaceous rocks (Figure 15). This unit is characterized occasionally by continuous but mostly semi-continuous by low to high amplitude reflectors. Thickness within the study area increases toward the southeast. The Molassic sediments here consist predominantly of siliciclastic sediments consisting of intercalated sandstones, marl and marly sandstone. The upper part consists of marl and sandstone (freshwater Molasse) while the lower section consists of marl, sandstone, limestone and (lower Molasse) and Gompholites (excluding GEO-02 area) at the very base of this unit (Figure 10). Importantly in the GEO-02 a ca 130 thick Siderolithic unit was penetrated just above the Lower Cretaceous (Figure 10).

7.2. Well Correlation between GEO-01 and GEO-02

Well correlation between GEO-01 and GEO-02 boreholes located 6956 m apart reveal the stratigraphic architecture of the Geneva Basin can change over a relatively short extent (Figure 10). Although the GEO-02 is deeper penetrating the upper Jurassic sequence, there exist a thicker Cenozoic sedimentary cover in the GEO-02 compared to GEO-01. This is principally associated with general dipping the geologic layers from N to S and with the discovery of 140 m thick Siderolithic layer in GEO-02 not existent in GEO-01.

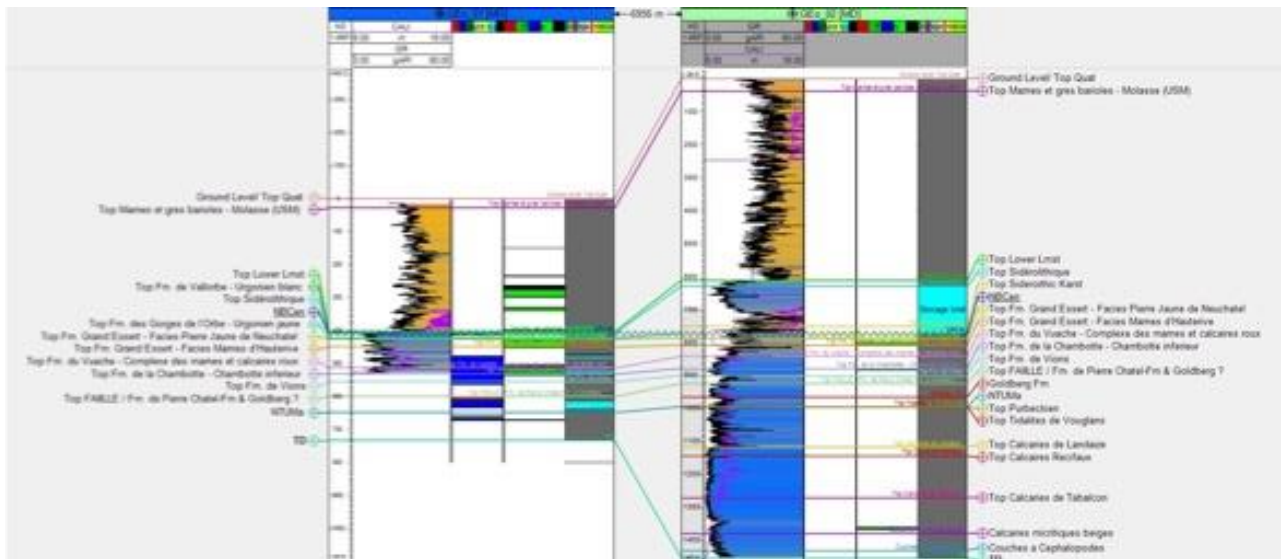


Figure 10 Well log correlation between GEO-01 and GEO-02 showing the respective formation encountered. Note the Siderolithique unit only exists in GEO-02. Faulted (red frame) and fractured (blue frame) intervals are also indicated. Intervals with light hydrocarbon (green frame) and bitumen (black frame) are also indicated in the fluid panel.

7.3. Seismic Interpretation

7.3.1. Seismic Interpretation 1 at GEO-01

Seismic line GG 87-02 reveal a prominent flower structure cross-cutting the Dogger, Malm, the Lower

Cretaceous carbonates and part of the Lower Molasse sediments (Figure 10). This flower structure consists of four NW-SE dipping strike-slip faults and two NE-SW dipping strike-slip faults (Moscariello et al., 2019a). Some of these faults accommodate small vertical throw that affects the Lower Cretaceous carbonates. The strike of the faults is assumed to be ENE-WSW (068°), considering a likely alignment parallel to the Jura chain (Moscariello et al., 2019). Similar structural trends have been documented in the Geneva Basin (Gorin et al., 1993, Signer and Gorin 1995; Clerc et al., 2015). We suspect some traces of the first two northwesternmost faults observed on the line GG 87-02 can be traced on the other line promoting the establishment of the fault planes and deducing a SW-NE trend for both faults. Based on this, and knowledge of the geological setting together with synthesis from the literature, we hypothesize this trend for the remaining faults. Importantly, many smaller-scale deformations are mappable in the Cenozoic sediment, however, due to the chaotic nature of the seismic facies here, they are difficult to establish (Figure 11).

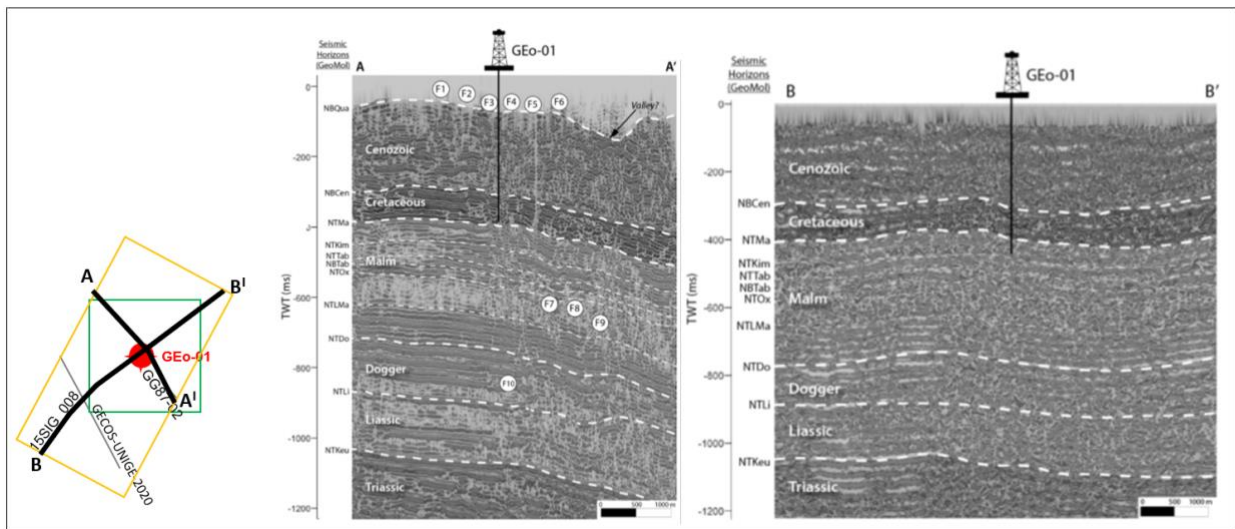


Figure 11 Seismic interpretation 1 of Line GG87-02 and 15 SIG.

7.3.2. Seismic Interpretation 2 at GEO-01

In this scenario a flower structure is interpreted deforming the entire stratigraphy from the Cenozoic to the Triassic succession (Figure 11). Here, four strike slip faults have been interpreted, two dipping NW-SE, while the others dip NE-SW on line GG 87-02 Figure 8). However, compared to seismic interpretation 1, these strike-slip faults are oriented in opposing direction trending WNW-ESE (Figure 11).

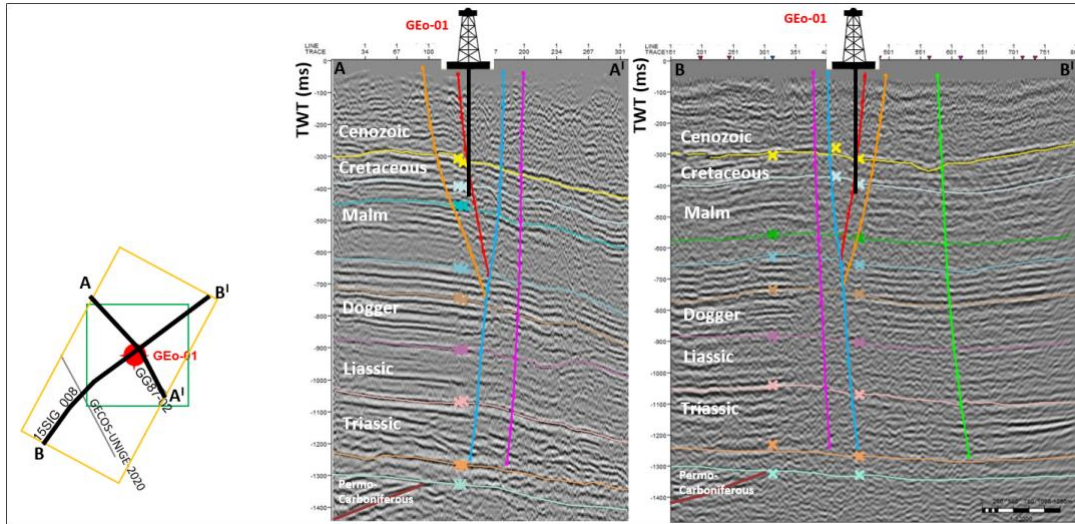


Figure 12 Seismic interpretation 2 of line GG87-02 and 15 SIG.

7.3.3. Seismic Interpretation 3 at GEO-01 using the GECOS-UNIGE-2020 Line

Addition of the GECOS-UNIGE-2020 Line has permitted a third plausible subsurface structural scenario around the GEO-01 area (Figure 13). Here, a main thrust fault is introduced deforming the Molasse to the Triassic succession into the seismic interpretation in addition other antithetic faults (Figure 14). Also, a shallower low angle trust fault with a decollement in the top Malm (Near Top Upper Malm Horizon) deforming the Lower Cretaceous Carbonates (Figure 9). Orientation of these faults is similar to those of seismic interpretation 2 (WNW-ESE). Importantly, this interpretation is also plausible based on the expression of a minor molasse hill in the topography likely related to the activity of the main thrust fault interpreted in the seismic profile (Figure 12).

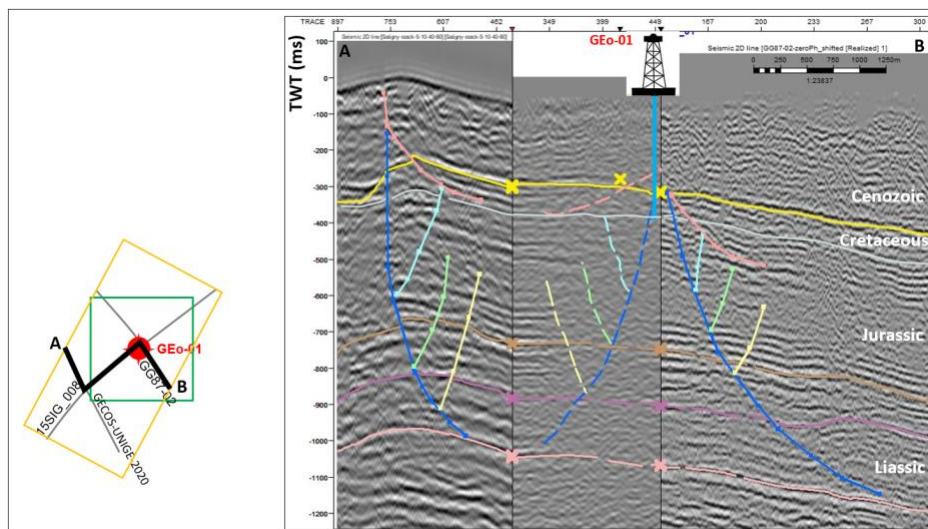


Figure 13 Seismic interpretation 3 of composite line encompassing GG87-02 and 15 SIG and the new GECOS-UNIGE-2020

7.3.4. Seismic Interpretation 1 at GEO-02

The initial pre-drill structural interpretation derived from Clerc 20xx, cropped to the area of interest for GEO-02 suggest five N-S striking and W- E dipping thrust faults system and a normal fault deforming the Jurassic to Cenozoic sediments (Figure 14).

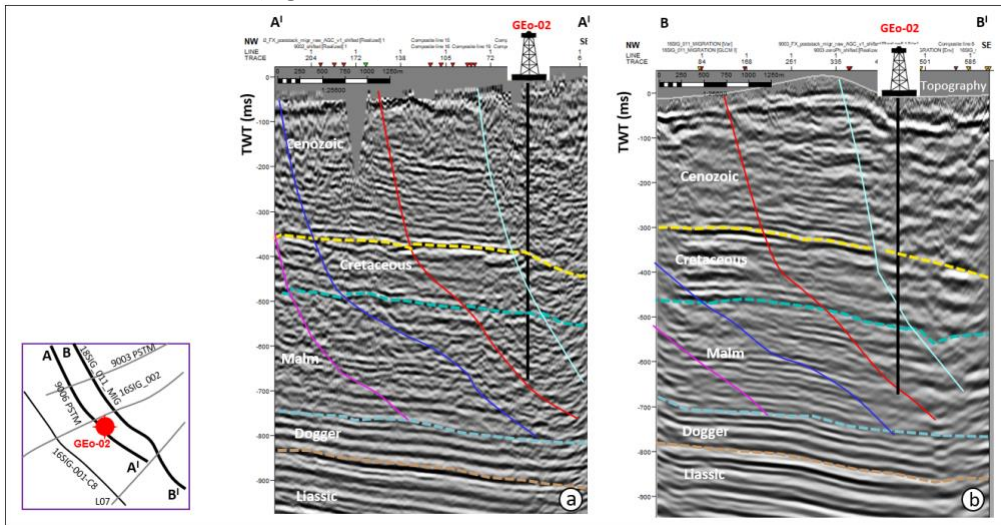


Figure 14 Seismic interpretation 1 of line 9006 PSTM and 18SIG_011_MIG

7.3.5. Seismic Interpretation 2 at GEO-02 including newly reprocessed data

However, integration of the reprocessed lines suggests a different structural organization in the GEO-02 area (Figure 15). Here a major thrust fault striking W-E and dipping N-S is interpreted and modelled alongside at least three other major faults likewise deforming the Jurassic to Cenozoic sediments (Figure 15). Importantly, unlike the predrill interpretation in Figure 11, here we combine the well data available from GEO-02 to interpret the presence of a Siderolithic unit which we hypothesize is fault-controlled. Here is also a high uncertainty associated with extent of this Siderolithic unit away from the borehole as demonstrated in Figure 15b1 and Figure 15b. The complexity of accurately interpreting this unit is also related to its thick with is just about 130 m and corresponding to less than 2 reflections event based on the resolution of the seismic dataset.

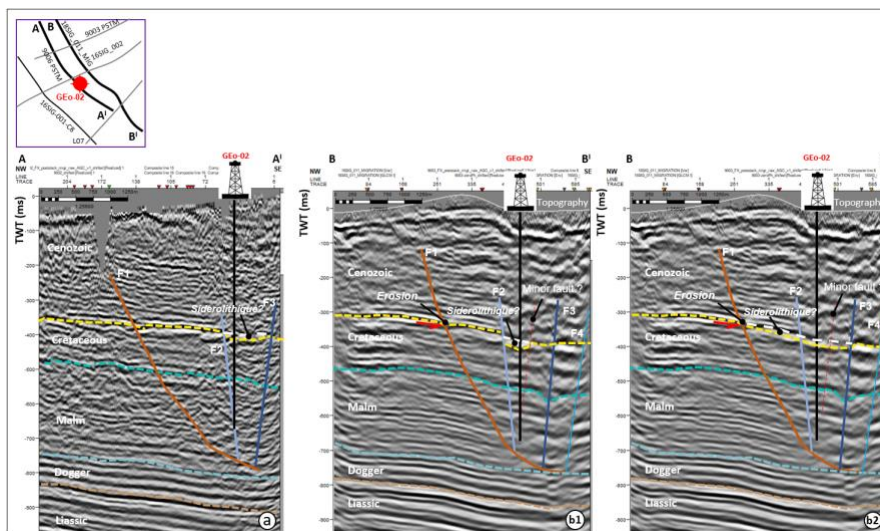


Figure 15 Seismic interpretation 1 of line 9006 PSTM and 18SIG_011_MIG. The Siderolithic unit above the Cretaceous unit has been interpreted with high uncertainty in two possible ways.

7.3.6. Petrophysical characters of the Lower Cretaceous Unit (main geothermal reservoir unit) for GEO-01 and Cretaceous and Jurassic geothermal reservoir for GEO-02

Integration of the well logs and drill cutting analysis and sedimentological analysis provided in the drilling/logging reports resulted in the identification of different lithofacies in the Lower Cretaceous interval (Figure 7). Most of the units are carbonate facies consisting of an alternation bioclastic limestone, peloidal bioclastic limestone, Marly limestone, Oolitic limestone, Oo-bioclastic limestone, Micritic limestone and Ooid-Peloidal bioclastic limestone. However sandy marl and marl occurs in the upper and lower segment of the of the Grand Essert Formation (Figure 10).

Log-derived petrophysical properties such as porosity and permeability are not reliable from GEO-01 since the calliper log reveal borehole deterioration over a large section of the well bore (Figure 10).

In order to achieve a robust estimate of this key petrophysical parameters, we compile values of core plug measurements from borehole penetrating similar formation in wells close to the present study area in the Geneva Basin. Generally, the entire Cretaceous intervals can be classified and tight having low porosity and permeability values ranging between 0.36 - 6.97 % and 0.002 - 0.107 mD (Rusillon and Chablais, 2017). However, the presence of faulted and fractured intervals and even karstification is prevalent in some of the formations which may promote localized enhancement in the petrophysical properties (Figure 11). In this study, we used a porosity value of 2 % for the Cretaceous unit, however, intervals with an aquifer was assigned a porosity value of 20%. A permeability value of 0.02 mD was assigned to the Cretaceous units while a value of 10 mD was used for intervals with an aquifer.

7.4. 3-D Geological Model Development

7.4.1. GEO-1 Area

Using the volume-based modelling approach the dimensions of the different geological models developed of at least 2 km x 2 km is deemed sufficient to understand the fate of the thermal plume, boundary condition and contain any envisaged injector-producer well configuration/geometry during future dynamic simulations. Since the GEO-01 borehole encountered aquifers in the Lower Cretaceous fractured Carbonate rocks the temporal limit of the model was set t to at least a temporal level within the Malm for Model 1, base Permo-Carboniferous for Model 2 (based on the deep strike-slip fault system modelled) and finally for Model 3 up to the base Mesozoic (Figure 16). The dimensions of the three models are as follows (excluding the overburden and Underburden added to the modelling process):

GEO-01 3D Geological Model 1 has a volume of 2 km x 2 km x ca. 2.63 km terminating in within the Keuper (Figure 14). Main fault trend in this model is ca. NE-SW (Figure 14). GEO-01 3D Geological Model 2 has a volume of 2 km x 2 km x 3.17 km. Main fault trend is nearly WNW-ESE. New Permo-Carboniferous graben was modelled using a velocity of 4 km/s. GEO-01 3D Geological Model 3 has a volume of 2 km x 2 km x 3.83 x 3.04 km. the newly acquired 2d seismic line across Satigny February 2020. Main fault trend is WNW-ESE. This model terminates at Base Mesozoic.

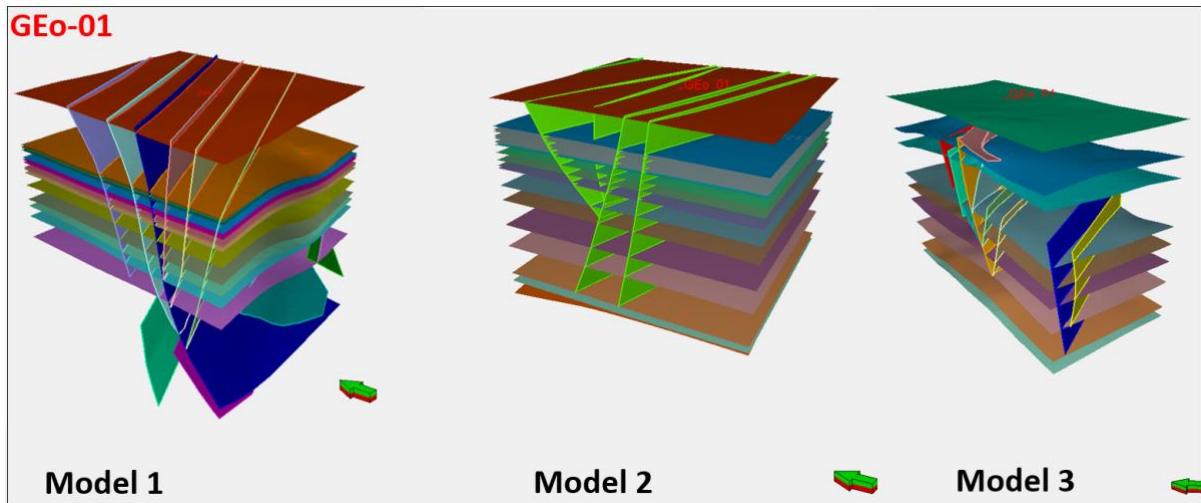


Figure 16 fault model and horizon model for the three different seismic interpretation or GEO-01.

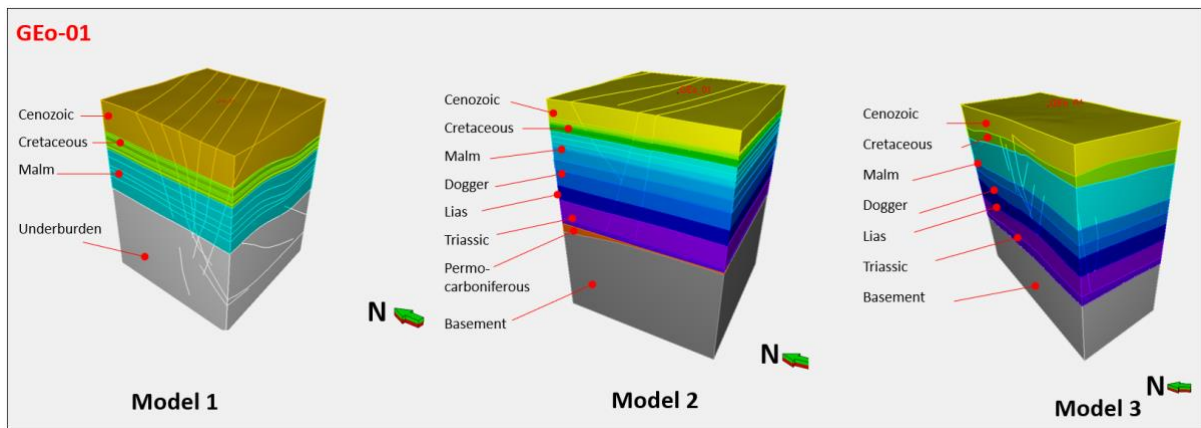


Figure 17 Geological model for the three different structural and stratigraphic frameworks modelled or GEO-01.

7.4.2. GEO-2 Area

Two geological models GEO-02 Model 1 and 2 was developed for the Geo-02 area. GEO-02 Geological Model 1 and 2 has a volume of 2 km x 2 km x ca. 2.60 km at the Dogger unit beyond the total depth of the GEO-02 borehole (Figure 14). Fault structural and stratigraphic model 1 (Figure 15a), with the exclusion of the Siderolithic (Figure 19) since this was a pre-drill model (Figure 16) was used in building the geological model presented in Figure 20a.

GEO-02 Geological model 2 has the same dimensions as Geological model 1, however with a different structural and stratigraphic framework shown in Figure 15 Model 2 based on the seismic interpretation (Figure 12). Here the Siderolithic unit has been modelled as infilling a fault-controlled karst with a width of ca. 0.5 km, 0.95 km in length (crossing the two main seismic line 9006 PSTM and 18SIG_011_MIG where it has been interpreted) and depth of 130 m corresponding to the thickness of this unit. However, other possible geological scenarios of modelling the Siderolithic may exist as shown in Figure 16 a-c. However, in this study we limited ourselves to building the conceptual geological model presented in Figure 16a with reliable well control albeit with uncertainties in the width (Figure 16 d-e).

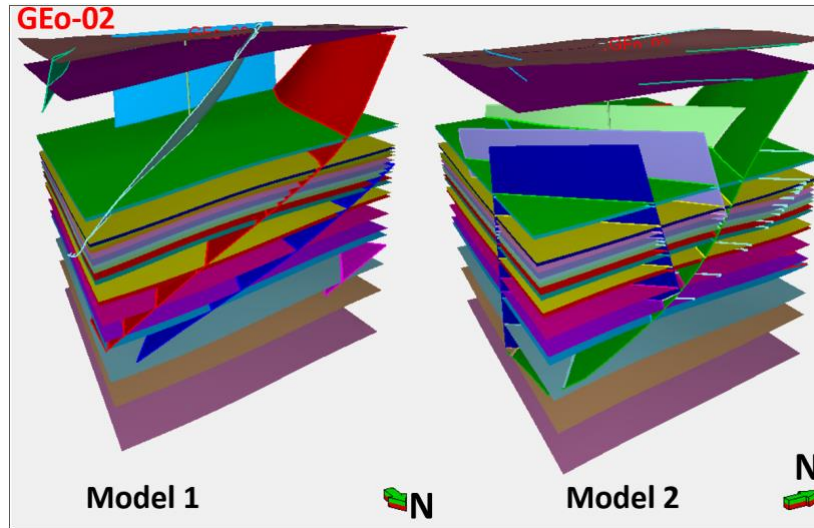


Figure 18 structural and stratigraphic framework derived from interpreting the seismic reflection dataset and layering using the formation top from GEO-02 borehole.

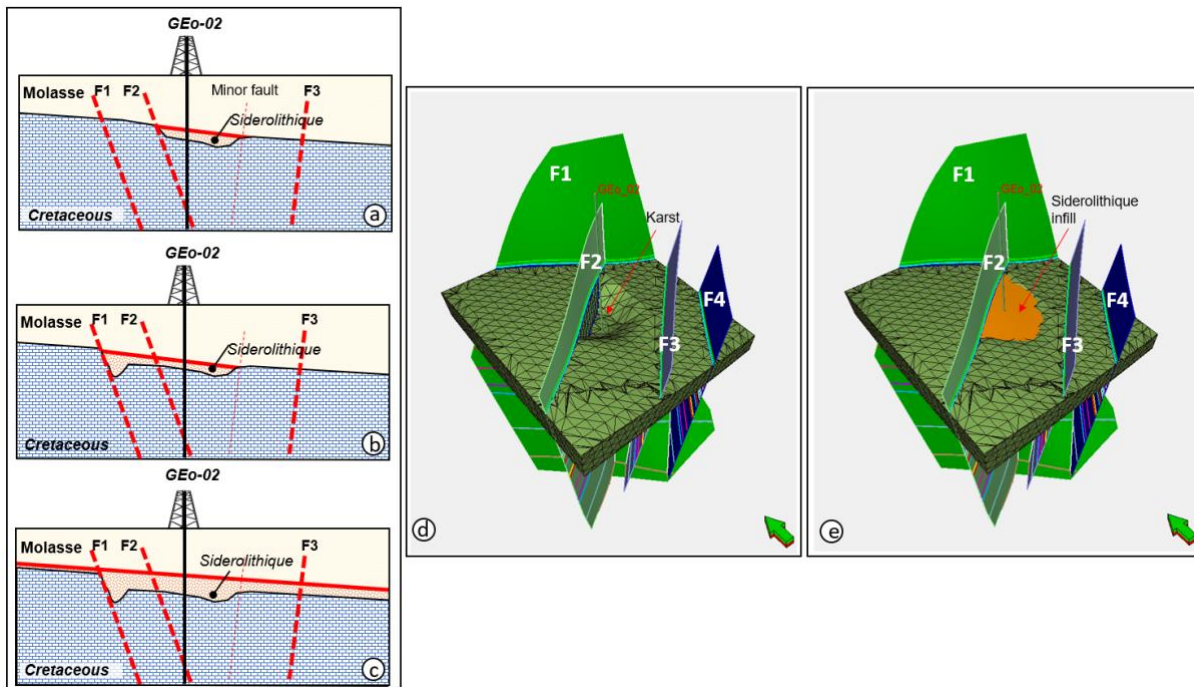


Figure 19 a-c. Conceptual geological sketches proposed for modelling the Siderolithic unit encountered by the GEO-01. (d) the simplest case of a fault-controlled karst development atop the Cretaceous unit was eventually used in this study, later infilled by the Siderolithic sediments as shown in Figure x.

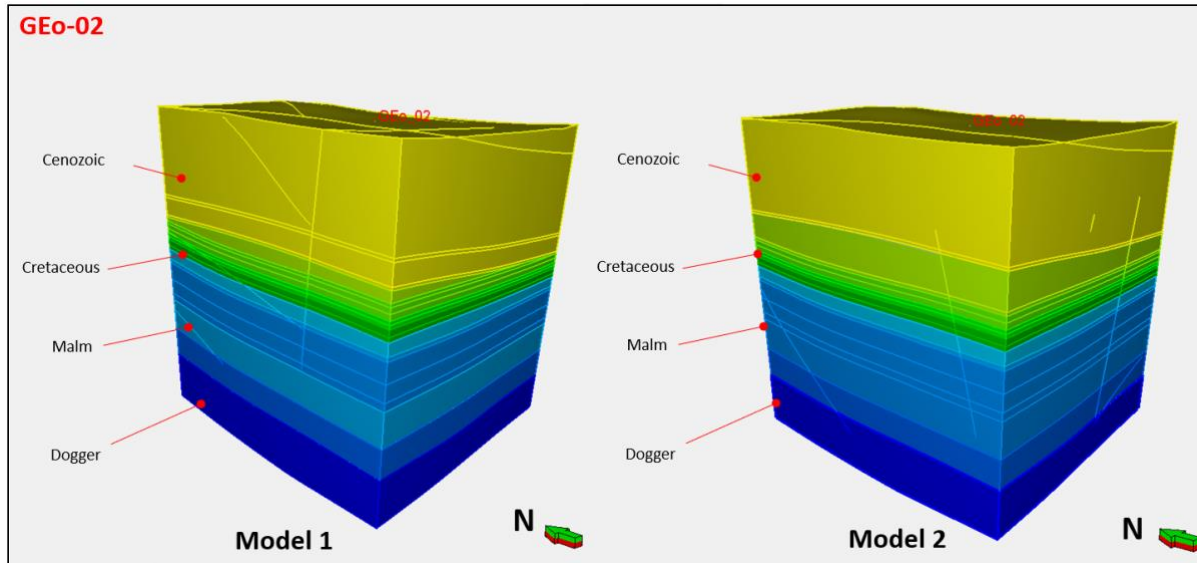


Figure 20 two different geological model (Model-1 and Model-2) developed for GEO 2 arising from the two different structural model used as input.

7.5. 3D static Modelling for the Cretaceous and Jurassic Reservoirs Across GEO-01 and GEO-02

7.5.1. GEO-01 Area

Integration of the well logs and drill cutting analysis and sedimentological analysis provided in the drilling/logging reports resulted in the identification of different lithofacies in the Lower Cretaceous interval (Figure 6). Most of the units are carbonate facies consisting of an alternation bioclastic limestone, peloidal bioclastic limestone, Marly limestone, Oolitic limestone, Oo-bioclastic limestone, Micritic limestone and Ooid-Peloidal bioclastic limestone. However sandy marl and marl occurs in the upper and lower segment of the of the Grand Essert Formation (Figure 21).

Log-derived petrophysical properties such as porosity and permeability are not reliable from GEO-01 since the calliper log reveal borehole deterioration over a large section of the well bore (Figure 21). In order to achieve a robust estimate of this key petrophysical parameters, we compile values of core plug measurements from borehole penetrating similar formation in wells close to the present study area in the Geneva Basin. Generally, the entire Cretaceous intervals can be classified and tight having low porosity and permeability values ranging between 0.36 - 6.97% and 0.002 - 0.107 mD (Rusillon and Chablais, 2017). However, the presence of faulted and fractured intervals and even karstification is prevalent in some of the formations which may promote localized enhancement in the petrophysical properties (Figure 21).

In this study, we used a porosity value of 2 % for the Cretaceous unit, however, intervals with an aquifer was assigned a porosity value of 20%. A permeability value of 0.02 mD was assigned to the Cretaceous units while a value of 10 mD was used for intervals with an aquifer. Several factors such as the sedimentary facies association, presence of faults, karst and fractures networks and importantly the occurrence of bitumen and light oil shows and the water flow from the aquifer were considered during the selection of potential candidate storage interval in the study area (Figure 21). In this study, we have discounted promising intervals with proven evidence of aquifers characterized by significant water outflow but less than 10 m thick and also evidence of hydrocarbons (Figure z). Following this, we have identified three candidate horizons in the Lower Cretaceous carbonates for HT-ATES development. The static model was developed using the preferred geological model 1.

- **Cretaceous Target 1 (CT1):** 10 m thick horizon in the Grand Essert Fm / Marnes d’Hauterives Fm. This interval is characterized by Bioclastic sandstone rich in peloids and bioclasts.
- **Cretaceous Target 2 (CT2):** 12.5 m thick interval in the uppermost part of the Vuache Fm - Chambotte- Chambotte inférieur. This interval is characterized by bioclastic sandstones, rich in peloids and bioclasts. Fractures are also present and white calcite veins (majority <5mm) (Figure z).
- **Cretaceous Target 3 (CT3):** The deepest horizon is a 25 m thick interval within the Goldberg Fm. The upper 13 m consists of bioclastic limestone while the lower 12 m is characterized by Oopelioidal limestone. This interval is faulted and fractured (Figure 21).

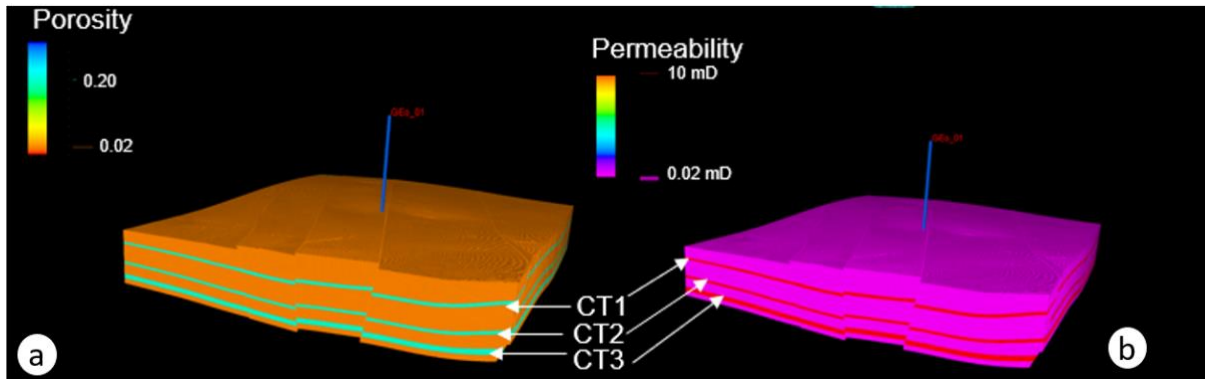


Figure 21 (a) Porosity and (b) permeability model for the cretaceous interval. Potential intervals are CT1, CT2 and CT3 within the Cretaceous.

7.5.2. GGeo-02 Area

Unlike the GGeo-01, analysis of the GGeo-02 from the well report and well test report revealed only the Eocene Siderolithique unit to be a potential storage interval (Figure z). Other expected units in the Cretaceous and Jurassic are tight with no significant water outflow. The Siderolithique unit is sand-rich infilling the karstified and fractured underlying erosional surface of the lower cretaceous. Log-derived petrophysical properties such as porosity and permeability were used for the lower-case range of petrophysical properties for this unit. The porosity was modelled using a porosity value of 10 % to 25 % for the entire Siderolithique unit, while a permeability distribution ranging between 5 – 300 mD was used in populating the static model (Figure 22). The static model was developed using the preferred geological model 2.

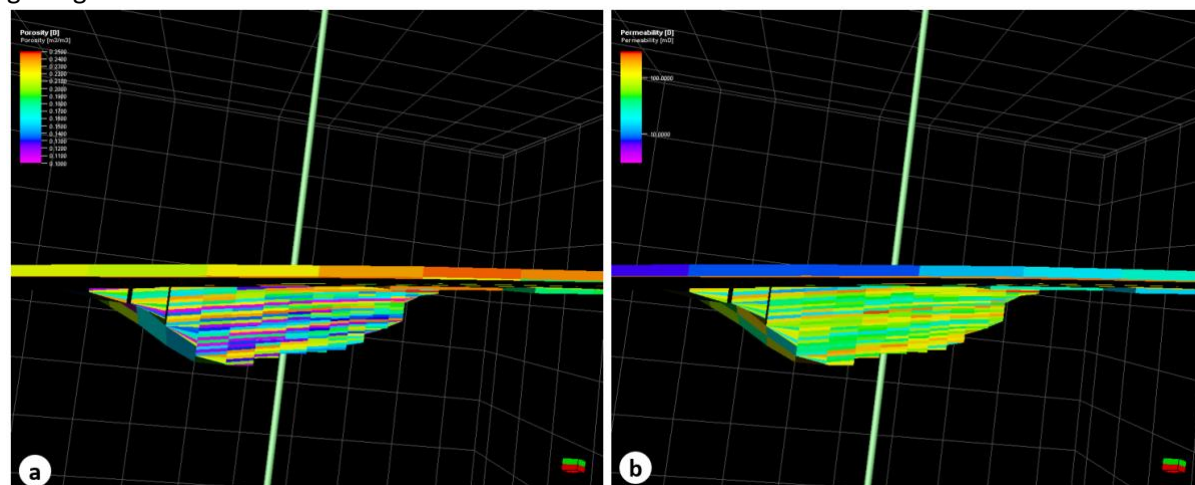


Figure 22 (a) Porosity and (b) Permeability modelling for the Siderolithique unit.

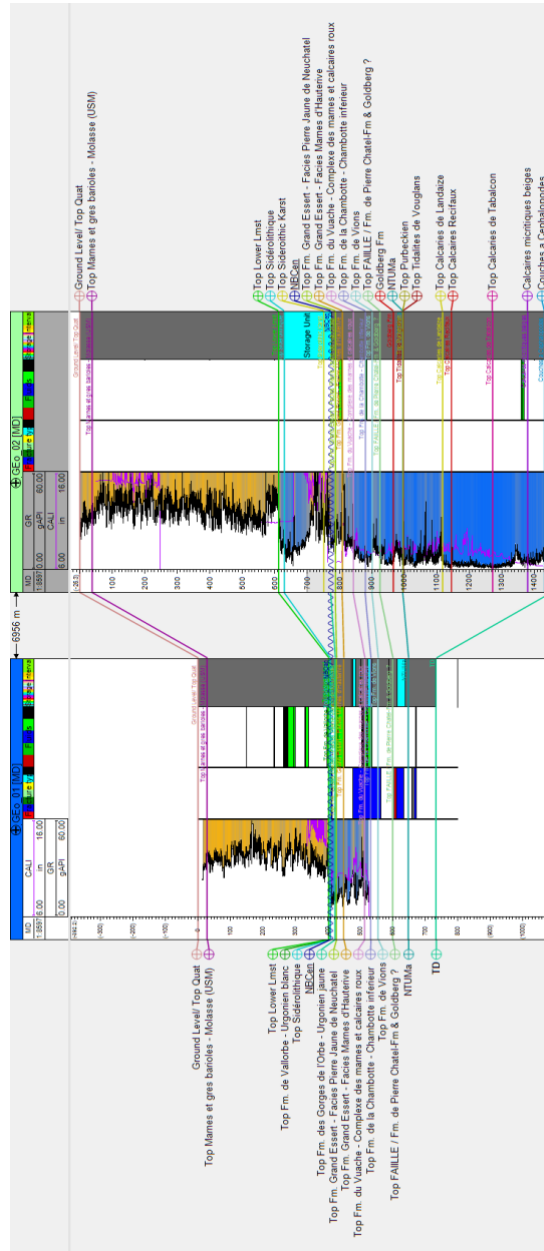


Figure 23 Well log correlation between GEO-01 and GEO-02 showing the respective formation encountered. Note the Siderolithique unit only exists in GEO-02. Faulted (red frame) and fractured (blue frame) intervals are also indicated. Intervals with light hydrocarbon (green frame) and bitumen (black frame) are also indicated in the fluid panel.

8. Discussions

8.1. Uncertainties associated with the 3-D Geological Model development around the GEO-01 and GEO-02 area

Associated with 3-D subsurface modelling is the problem of incomplete knowledge of the subsurface (Siler et al., 2019). The robustness of the 3-D static model developed here is dictated by the integration of the subsurface dataset, their interpretation, and associated uncertainties (Moscariello, 2016; Schweizer et al., 2017). A major factor contributing to this uncertainty is the density of the subsurface

dataset (2-D seismic reflection survey, borehole dataset) analysed in this study (Figure 8). Moreover, each of this dataset analysed is associated with some uncertainties related to its acquisition technique and data processing (Siler et al., 2019). This hold for the Geneva Basin since multiple vintages of 2D seismic reflection dataset exist. This has a ripple effect on the understanding of the structural configuration of the study area and the final model geometry. Also, in the 3-D geological models developed in this study, the farther the distance from the input dataset the greater the uncertainty in constraining the subsurface geology configuration. Following this, interpretation and modelling is more robust and better constrained near the GGeo-01 and GGeo-02 borehole.

Importantly, worth mentioning unequivocally is the ambiguous nature of seismic interpretation. This is more pronounced in fault interpretation and modelling (number of faults, fault orientation, fault length, fault height and type of fault contact in relation to a fault network) (Cherpeau et al., 2010; Julio et al., 2015; Røe et al., 2014) compared to horizon interpretation. Multiple fault interpretations for GGeo-01 and GGeo-02 are presented in this study to capture part of this uncertainty (Figures 8-12). Indeed, these fault interpretations and models presented here is geologically realistic and likewise plausible based on the tectonostratigraphic evolution of the study area (e.g. Gorin et al., 1993, Clerc et al., 2015; Moscariello et al., 2020). In this study, significant uncertainty is expressed in the length of the faults mapped and direction of the fault plane since this cannot be deduced based on the low density of the 2-D seismic profile analysed here (Figure 11- Figure 15 and Figure 20). Also, the extrapolation of this direction is based on a knowledge-driven hypothesis especially in the case of GGeo-01 which would be tested when 3-D seismic data becomes available in the Geneva Basin at the end of 2020. Further uncertainty is likewise demonstrated regarding modelling the Siderolithic deposits and what controlled the development of the karst in which these sediments are deposited and its volume (Figure 20).

The geometry of these faults mapped will ultimately have an implication on the performance of the ATES system in terms of storage volume and aquifer properties and any further discrete fracture network modelling. A major issue is a difficulty in mapping faults in the Molasse and Quaternary unit based on the chaotic nature of the seismic reflections (Figure 11-Figure 15).

Any perturbation in the subsurface configuration of the study area not captured by our interpretation due to the nature of the input dataset may also affect the dip and azimuth of key surfaces and storage intervals. This has implications on the thickness variation of the potential storage targets in the Lower Cretaceous, also in the estimation of the storage capacity of the ATES system and ultimately in understanding the fate of the geothermal plume. We believe the regional surfaces provided by the GEOMOL project ameliorates the uncertainty in the stratigraphic interpretation of the major units. Furthermore, the availability of formation tops from the GGeo-01 and GGeo-02, and importantly check-shot from GGeo-02 borehole allowed a local refinement of the interpretation derived from the GEOMOL project. Since we interpreted 2-D seismic profiles it was almost impossible to deduce lateral and temporal changes in seismic facies characteristic of different formations in areas distal to the input dataset. Only the GGeo-01 well and GGeo-02 was available within the region of interest introducing uncertainty during the facies modelling. Here, we assumed mostly a lateral homogeneity in the seismic facies in each formation or aquifer within the model boundary. While this may be far for the subsurface reality as demonstrated by the unexpected thickness of the Siderolithic sediments drilled in GGeo-02, we do not expect much variation in the Lower Cretaceous and Upper Jurassic since the carbonate facies may have little variation based on the scale of our model.

The (over)simplification of the facies model presented here assume localized homogeneity, this may affect the distribution of porosity and permeability with further implication on the behaviour of the geothermal plume. Importantly, the borehole logs available did not cover the entire interval due to hole

stability problem, leaving the evaluation of the unlogged intervals to be on the analysis of the borehole cutting recovered. While analysis of the drill cuttings is a robust methodology for characterizing facies, only their advanced analysis proffers a good match with log data to provide direct correlation with subsurface formation penetrated (Salim & Lagraba, 2018). Yet some bias cannot be totally neglected which may arise due to the drilling strategy and mixing of drilling samples may occur at deeper levels resulting in the obscuring of primary lithology (Fowler & Zierenberg, 2016).

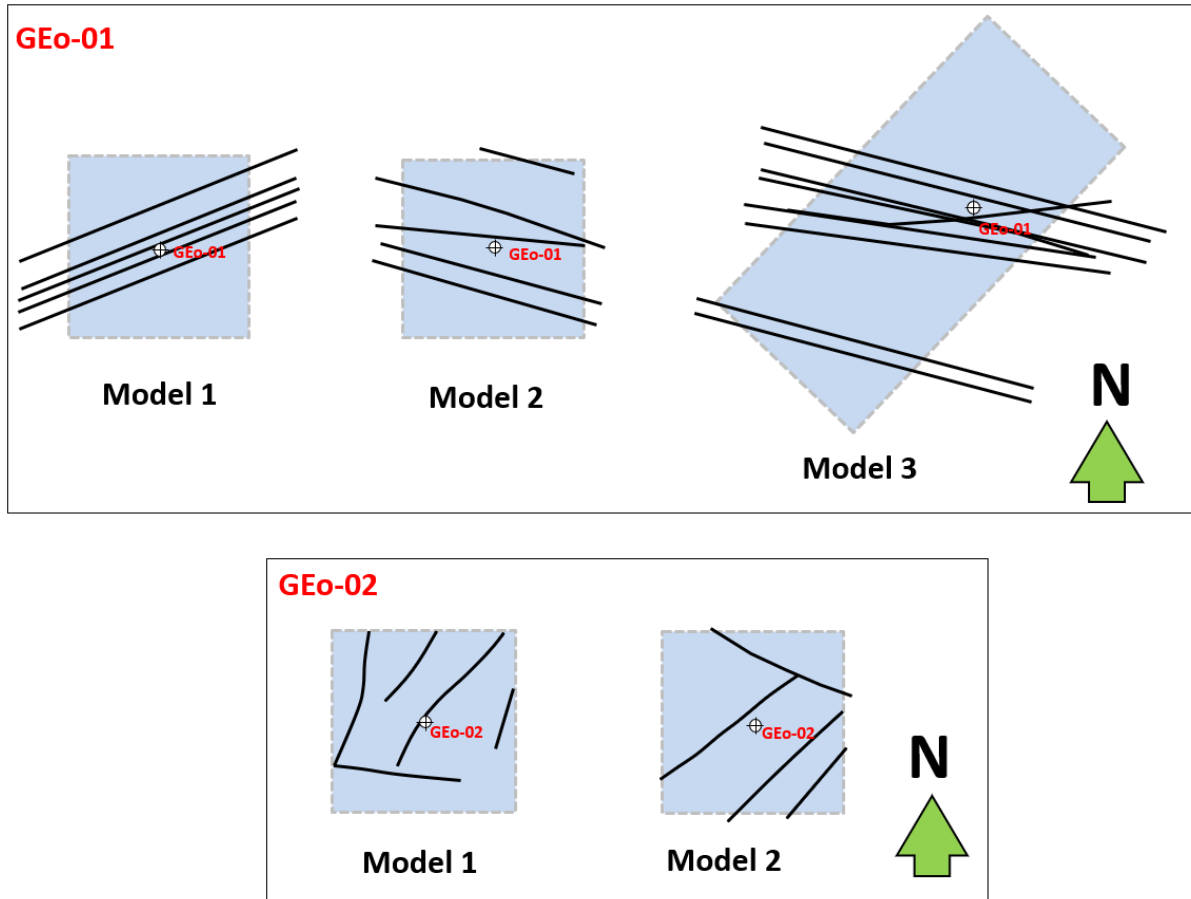


Figure 24 Different fault orientations from the different geological models developed (Model 1-3).

8.2. Impact of 3-D geological model, Petrophysical and facies properties on geothermal reservoir – Lower Cretaceous Unit

The impact of the geological features modelled in this study on geothermal reservoirs depends explicitly on the way it has been represented in the 3-D geological model built in this study (*sensu* Shekhar et al., 2014). Invariably it is related to the hypothesis and assumptions made to arrive at the closest match to the subsurface reality. For any geothermal development, the structural configuration related to the geo-history manifested as faults system and fracture network is perhaps the most important in order to unravel the nature of the subsurface fluid flow. Faults are crucial structures for the transport of fluids, solute, and energy (Lopez and Smith, 1995). The strike-slip faults related to the flower structure mapped here affects the Upper Jurassic, Lower Cretaceous and the lower part of the Molasse creating a structural complexity and potential damage with the possibility of fracture enhancement and flow within this region (Figure 8). Normal fault systems and strike-slip faults occupying in extensional and

transtensional domains serve as a conduit for fluid flow also in non-magmatic geothermal systems as is the case of the present study area (*sensu* Moeck 2014; Moeck and Beardsmore 2014). Yet, the ability of these fault planes to serve as pathways for fluid plumbing is strongly controlled by the stress conditions along with the different stratigraphic units, lithofacies, fault displacement and temperature (*sensu* Bjørlykke, 1993; Knipe & McCaig, 1994, Yielding et al., 2016). Indeed, fault stress analysis has not been conducted in this study, however, faults in predominately carbonate formation such as the Lower Cretaceous Unit is often thought to be conduits for fluid flow due to their brittle nature (Yielding et al., 2016). These faults may be a low permeability fault rock system due to the possibility of fault healing related to the chemical reactivity of carbonates even after their reactivation (see Yielding et al., 2016). Favourable fault transmissibility here will occur in areas where these faults have enough displacement and juxtapose different lithofacies within the Lower carbonate rocks. In all, this fault may have an implication in preferentially promoting the upwelling of the geothermal fluids. The dip of the faults mapped here are high and may influence fluid circulation at depth (*sensu* Grasby and Hutcheon 2001) while faults properties such as the length, depth, thermal conductivity, lateral gradient in heat flow and fault rock permeability will determine whether the thermal regime along these fault planes at the Cretaceous level is governed by advection or convection (*sensu* Lopez and Smith, 1995).

The carbonates in the Lower Cretaceous unit were deposited in a shallow water environment with lithofacies within the main target storage horizon either micritic limestone or bioclastic limestone. Petrophysical analysis on core samples within these intervals reveals a tight reservoir system with very low permeability and porosity however with intervals characterized by fractures and karsts and faults (Figure 6). Fractures and faults any fault depending on their properties may enhance flow within the aquifer, however, a major problem then will be injectivity into this tight carbonate system in the absence of the later. Lateral connectivity between this aquifer will depend on the facies variability. Since a minimal facies variability is expected within the study area storativity may be enhanced. This hypothesis of facies homogeneities is supported by the acoustic property of the Lower Cretaceous in the study area showing a little variation on seismic data except in highly deformed area. Other potential issues related to injectivity into this tight carbonate system is a potential for formation damage. This may arise and have an implication on the spatio-temporal mobility of the injected fluids.

8.3. Implication of hydrocarbon occurrence in the study area on geothermal development

The G_{EO}-01 and G_{EO}-02 borehole encountered hydrocarbons in some parts of the Molasse and the Lower Cretaceous unit (Figure 18). This is not unique in the Swiss Plateau as other Geothermal exploration boreholes - St Gallen GT-1 and Schlattingen likewise encountered hydrocarbons (Moscariello et al., 2020). Furthermore, gas seeps and bitumen seeps have likewise been documented in outcrops (Leu and Oester, 2012) pointing towards an active petroleum system (*sensu* Magoon and Dow, 1994). However, the generation and migration of hydrocarbons in the Swiss Molasse Basin are still not completely understood and currently under investigation (Schegg et al., 1999; Moscariello et al., 2019b). In this study, potential candidate storage horizons with the manifestation of light oil and heavy oil (bitumen) and even oil shows as documented in the drilling report have been identified as horizons of potential risk during the selection of suitable targets for geothermal production. Indeed, the production or injection of hot water into hydrocarbon-rich or bitumen impregnated intervals in the Lower Cretaceous will ultimately reduce the oil viscosity and mobility ratio resulting in enhanced oil recovery (*sensu* Prats, 1986; Bousaid, 1991; Jabbour et al., 1996 and Okasha et al, 1998). This scenario is plausible since the Lower Cretaceous unit is highly faulted and fractured These faults systems and fracture network depending on their hydraulic behaviours may act as either high-permeability conduits for

channelling these hydrocarbon-contaminated-water to the storage intervals and even towards shallower siliciclastic molassic intervals where they may be sequestered or rather behave as barrier or mixed conduit-barrier system (sensu Aydin 2000; Bense et al. 2013; Caine et al. 1996; Faulkner et al. 2010). Without these deformation pathways, the likelihood of cross-strata or cross formational geothermal fluids breakthrough is limited since the porosity of the Mesozoic series and even the molassic sediments is low (Brink et al., 1992; Kälin et al., 1992) and characterized by a complex mix of sediments (Schegg et al., 1999). Therefore, the occurrence of hydrocarbons remains a potential risk for the successful development of ATEs in this portion of the Swiss Molasse Basin. Considering this, some authors have suggested the possibility of co-producing the geothermal and hydrocarbon resources in the Swiss Molasse Basin (Moscariello et al., 2018).

9. Conceptual model evaluating the storage potential of the study area

Based on the configuration 3D geological models developed for the G_{Eo}-01 and G_{Eo}-02 and synthesis of information from literature, multiple geothermal exploration scenarios and hypothesis on the long-term fate of the geothermal fluids in the Lower Cretaceous and Upper Jurassic can be tested. Here, we consider the G_{Eo}-01 and G_{Eo}-02 well as producer only and the location of a second well that will compose the doublet potentially in future operation will be defined by the dynamic reservoir modelling (Birdsell & Saar, 2020; Mindel & Driesner, 2020, Figure 24). Despite being based on a simplified structural model, we can anticipate that the fate of the geothermal production can be sustainable in the long terms due to the high flow rate and pressure observed at the well head.

The Lower Cretaceous and Upper Jurassic is in generally has a tight matrix system characterized by low porosity, low permeability, but, locally, karst and fractured networks associated with brittle structures dramatically increase porosity and permeability (Figure 18). Here the fault networks modelled results in natural upwelling of groundwaters (Figure 18). The preferential migration of fluids upwards along the fault system can be enhanced or even represent an element of risk if the reinjection is operated upstream at a distance from the production well not adequate to balance the local depressurization of due to the production. The presence of a highly conductive fault zone controlling the natural artesian flow observed at G_{Eo}-01 is a challenge as the optimal distance between production and reinjection wells must be identified in order to sustain the production, avoiding excessing increase in pressure. Drilling report corroborates a fault-controlled system in the vicinity of the G_{Eo}-01 well, with a high-velocity flow at the wellhead recording a similar temperature as the aquifer temperature (Guglielmetti, 2020). At G_{Eo}-02 the permeability of the carbonate reservoirs has been proved to be very low, indicating a clear compartmentalization between the G_{Eo}-01 and G_{Eo}-02 areas, most probably also controlled by the different structural configuration of the fault structures that characterize the two sites. The natural recharge of the system here is from the Jura Mountain chains (Figure 5) and circulation at depth is related to the hydraulic gradient. The faults encountered in the Lower Cretaceous and Upper Jurassic are open strike-slip faults and G_{Eo}-01 laterally confining and vertically promoting localized fluid circulation, and tight thrust structures at G_{Eo}-02 acting rather as a barrier for fluid flow. Since no aquifer was encountered in the Oligocene Molassic sediments, albeit deformed and characterized by faults extending from the Lower Cretaceous, we suggest this unit seals the entire system. The lithofacies property of the Molasse especially the increase in the shaliness may have downgraded the plumbing capability of the faults here (Figure 10).

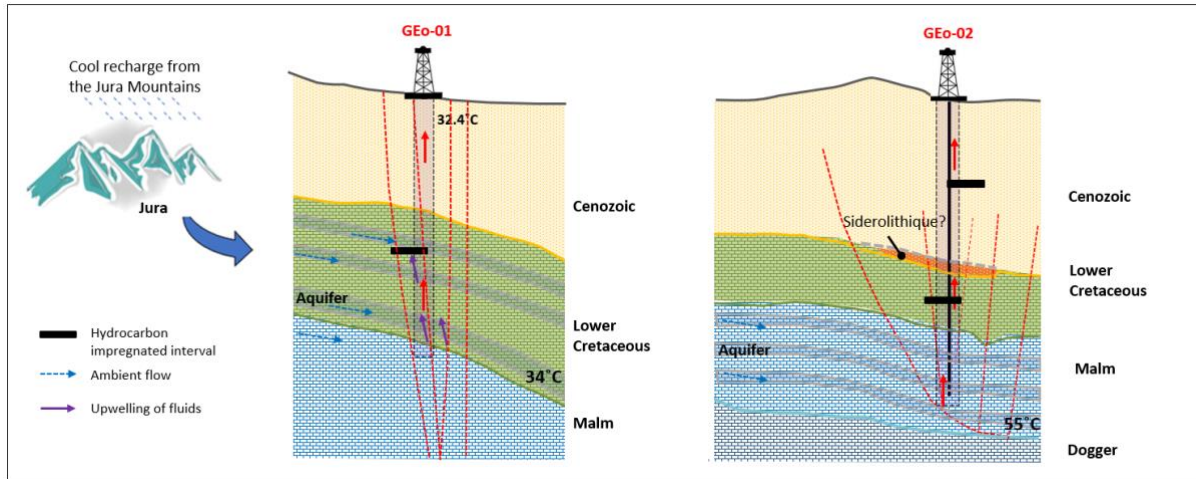


Figure 25 Conceptual model showing the fate of the thermal plume based on the GEO-01 well assuming high-temperature fluids are injected in the thickest and deepest aquifer CT3 in the Grand Essert formation.

10. Conclusions

In this contribution, we present the workflow and results for the development of a geologically realistic 3-D static model in a geothermal perspective based on the integration of a suite of subsurface geophysical dataset around the GEO-01 and GEO-02 geothermal exploration borehole recently drilled in the Geneva Basin. Start-of-the-art volume-based modelling technique has proved successful in developing a stable and robust sets of 3D geological models when combined with knowledge-driven modelling decisions to ameliorate for areas with low data density inputs.

However, uncertainties remain especially in the fault geometry and modelling and facies distribution which was assumed to be homogenous in this simplistic case presented here. This is further supported by the discovery of the Siderolithic sediments in GEO-02 which was not encountered in GEO-01. Petrophysical analysis suggests the Lower Cretaceous formations are tight, generally characterized by low porosity and permeability values (Moscariello et al., 2020). However, well test results highlight how the presence of a karstified, faulted and fractured intervals in the Lower Cretaceous and Upper Jurassic unit locally enhance porosity and permeability allowing large groundwater flows in GEO-01. This makes GEO-01 suitable for direct uses but very challenging for heat storage solutions due to the artesian flow condition and rather high wellhead pressure (8bars) and flow rate (50l/s). GEO-02 cannot be considered, at present commercially interesting for direct uses, due to very low flow rate (0.3 l/s) but could be suitable for storage in the Mesozoic carbonates only if permeability conditions can be enhanced if reservoir stimulations activity would be performed and will be successful. However, the Siderolithic unit, might present suitable conditions for storage if a side-track well would be considered as an option in the future.

Additionally, the presence of light hydrocarbons and their heavier counterpart is an element that must be considered to identify future targets and plan production operations since they may reduce the oil viscosity and promote oil mobility resulting in enhanced oil recovery. Therefore, the subsurface manifestation of hydrocarbon in the Lower Cretaceous in GEO-01 and GEO-02 remains a potential risk worth considered during further numerical modelling and development of deep geothermal projects and other geo-energy related projects in the Geneva Basin.

The structural situation around GEO-01 and GEO-02 area, especially the occurrence of a rather large fault

structures, EW oriented in G_{Eo}-01 may have implications on the definition of the drilling and operation strategies at these sites. While the faults networks associated with the flower structure modelled in G_{Eo}-01 here promote a preferential vertical accent of the geothermal fluid flow, the distribution of the fault-rock properties across its entire volume might show lateral and vertical heterogeneities that have to be considered for future industrial developments. This will be controlled by different aspects of basin geohistory, lithofacies, stress and fault displacement and the behaviour of the fracture networks in the Lower Cretaceous series. This is beyond the scope of the present study and will be considered as future directions.

In the future development of geothermal projects in the study area, but more in general in the Geneva basin, strike-slip fault structures will represent the main geothermal target to be considered. Yet a multi-horizon development strategy based the distribution of the fault properties can be considered but to produce models able to include such elements 3D high resolution data, such as the 3D seismic survey planned by Q4 2021 by SIG, will need to be acquired. This would permit testing the validity of our mostly knowledge-driven fault model presented for the faults orientation in both G_{Eo}-01 and G_{Eo}-02 area and in understanding the Siderolitic deposit around the G_{Eo}-02 Area Until then, the models presented here is only the first attempt of a finer-scale representation of the subsurface geology with requisite characteristics and parameters for understanding the development of an ATES system in the Geneva Basin. Importantly, our findings highlight the urgent need for subsurface data augmentation in the study area, especially in the light of ongoing and future geothermal exploration campaign in the Geneva Basin.

REFERENCES

- Aydin, A., 2000. Fractures, faults and hydrocarbon entrapment, migration and flow. *Mar.Pet. Geol.* 17, 797–814.
- Bárdossy, G. and Fodor, J., 2004. Review of the Main Uncertainties and Risks in Geology. *Evaluation of Uncertainties and Risks in Geology.*
- Becker, D., Rauber, G. and Scherler, L. (2013) 'New small mammal fauna of late Middle Eocene age from a fissure filling at la Verrerie de Roches (Jura, NW Switzerland)', *Revue de Paleobiologie*, 32(2), pp. 433–446.
- Bense, V.F., Gleeson, T., Loveless, S.E., Bour, O. and Scibek, J., 2013. Fault zone hydrogeology. *Earth-Science Reviews*, 127, pp.171-192.
- Birdsell, D. T., & Saar, M. O. (2020). Modeling Ground Surface Deformation at the Swiss HEATSTORE Underground Thermal Energy Storage Sites. World Geothermal Congress 2020. Reykjavik, Iceland: Submitted for publication.
- Bloemendal, M., Olsthoorn, T. and Boons, F., 2014. How to achieve optimal and sustainable use of the subsurface for Aquifer Thermal Energy Storage. *Energy Policy*, 66, pp.104-114.
- Bousaid, I.S. and Others, 1991. Hot-water and steamflood studies using kern river oil. In: *SPE International Thermal Operations Symposium*. Society of Petroleum Engineers.
- Brink, H. J., Burri, P., Lunde, A., & Winhard, H. (1992). Hydrocarbon habitat and potential of Swiss and German Molasse Basin: a comparison. *Eclogae Geol. Helv.*, 85, 715-732.
- Caers, J., 2011. *Modeling Uncertainty in the Earth Sciences*. John Wiley & Sons.
- Caine, J.S., Evans, J.P., Forster, C.B., 1996. Fault zone architecture and permeability structure. *Geology* 24, 1025–1028.
- Chablais, J. (2019). Forage Géo-01 Satigny (Genève) GEothermie 2020 : Résultats du 1er forage de prospection à Satigny (OPS & hydrogéologie). *Proceed Journée Romande de Geothermie*. Lausanne.
- Charollais, J.J., Weidmann, M., Berger, J.P., Engesser, B., Hotellier, J.F., Gorin, G.E., Reichenbacher, B. and Schäfer, P., 2007. La Molasse du bassin franco-genevois et son substratum. *Archives des Sciences*, 60, pp.59-174.
- Cherpeau N, Caumon G, Lévy B. Stochastic simulations of fault networks in 3D structural modeling. *C. R. Geosci.* 2010 Sep 1;342(9):687–94.
- Clerc, N., Rusillon, E., Moscariello, A., Renard, P., Paolacci, S. and Meyer, M., 2015. Detailed structural and reservoir rock typing characterisation of the Greater Geneva Basin, Switzerland, for geothermal resource assessment.
- Dickinson, J.S., Buik, N., Matthews, M.C. and Snijders, A., 2009. Aquifer thermal energy storage: theoretical and operational analysis. *Geotechnique*, 59(3), p.249.

Faulkner, D.R., Jackson, C.A.L., Lunn, R.J., Schlische, R.W., Shipton, Z.K., Wibberley, C.A.J., Withjack, M.O., 2010. A review of recent developments concerning the structure, mechanics and fluid flow properties of fault zones. *J. Struct. Geol.* 32, 1557–1575.

Fiore J, Girardclos S, Pugin A, Gorin G, Wildi W. 2011. Würmian deglaciation of western Lake Geneva (Switzerland) based on seismic stratigraphy. *Quaternary Science Reviews*, 30: 377-393.

Fowler, A.P. and Zierenberg, R.A., 2016. Geochemical bias in drill cutting samples versus drill core samples returned from the Reykjanes Geothermal System, Iceland. *Geothermics*, 62, pp.48-60.

Goodyear, S.G., Reynolds, C.B., Townsley, P.H., Woods, C.L., and Others, 1996. Hot water flooding for high permeability viscous oil fields. In: *SPE/DOE Improved Oil Recovery Symposium*. Society of Petroleum Engineers.

Gorin, G.E., SIGNER, C. and AMEERGER, G., 1993. Structural configuration of the western Swiss Molasse Basin as defined by reflection seismic data *Eclogae Geologicae Helvetiae*, 88, pp. 235–265.

Grasby, S.E. and Hutcheon, I., 2001. Controls on the distribution of thermal springs in the southern Canadian Cordillera. *Canadian Journal of Earth Sciences*, 38(3), pp.427-440.

Greber, E., Leu, W., Schegg, R., 1997. An evaluation of the oil and gas potential of Switzerland based on public well data, seismic lines and basin modelling results. *Geoform*, internal report. p. 107

Guglielmetti L., Eichinger F., Moscariello A., 2020. Geochemical Characterization of Geothermal Waters Circulation in Carbonate Geothermal Reservoirs of the Geneva Basin (GB). *Proceedings World Geothermal Congress 2020, Reykjavik*

Hooker, J.J. and Weidmann, M., 2007. A diverse rodent fauna from the middle Bartonian (Eocene) of Les Alleveys, Switzerland: snapshot of the early theridomyid radiation. *Swiss Journal of Geosciences*, 100(3), pp.469-493.

Hulen, J.B. and Sibbett, B.S., 1981. Sampling and interpretation of drill cuttings from geothermal wells. *DOEEETP (USDOE Office of Energy Efficiency and Renewable Energy Geothermal Tech Pgm)*.

Jabbour, C., Quintard, M., Bertin, H., and Robin, M., 1996. Oil recovery by steam injection: three-phase flow effects. *Journal of Petroleum Science & Engineering*, 16 (1), 109–130.

Julio C, Caumon G, Ford M. Sampling the uncertainty associated with segmented normal fault interpretation using a stochastic downscaling method. *Tectonophysics*. 2015 Jan 12; 639:56–67.

Kälin, B., Rybach, L. and Kempter, E.H.K., 1992. Rates of deposition, uplift and erosion in the Swiss molasse basin, estimated from sonic and density logs. *Bulletin der Vereinigung Schweizerischer Petroleum-Geologen und-Ingenieure*, 58(133), pp.9-22.

Karner, G.D. and Watts, A.B., 1983. Gravity anomalies and flexure of the lithosphere at mountain ranges. *Journal of Geophysical Research: Solid Earth*, 88(B12), pp.10449-10477.

López, D.L. and Smith, L., 1995. Fluid flow in fault zones: analysis of the interplay of convective circulation and topographically driven groundwater flow. *Water resources research*, 31(6), pp.1489-1503.

Magoon, L.B. and Dow, W.G., 1994. The petroleum system: chapter 1: Part I. Introduction.

Makhloufi, Y., Rusillon, E., Brentini, M., Moscariello, A., Meyer, M., & Samankassou, E. (2018). Dolomitization of the Upper Jurassic carbonate rocks in the Geneva Basin, Switzerland and France. *Swiss Journal of Geosciences*, 111(3), 475–500. doi:10.1007/s00015-018-0311-x

Mindel, J., & Driesner, T. (2020). HEATSTORE: Preliminary Design of a High Temperature Aquifer Thermal Energy Storage (HT-ATES) System in Geneva Based on TH Simulations. *World Geothermal Congress 2020, Reykjavik, Iceland: Submitted for publication.*

Misch, D., Leu, W., Sachsenhofer, R. F., Gratzner, R., Rupprecht, B., & Bechtel, A. (2017). Shallow hydrocarbon indications along the alpine thrust belt and adjacent foreland basin: distribution and implications for petroleum exploration. *Journal of Petroleum Geology*, 40(4), 341-362.

Moscariello A. Reservoir geo-modeling and uncertainty management in the context of geo-energy projects. *Swiss Bull. angew. Geol.* 21/1, (2016), 29-43.

Moscariello A. Guglielmetti L., Omodeo-Salé S., De Haller A., Eruteya O.E., Lo H.Y., Clerc N., Makloufhi Y., Do Couto D., Ferreira De Oliveira G. Perozzi L., DeOliveira F., Quiquerez L. Nawratil De Bono C., Meyer M.: Heat production and storage in Western Switzerland: advances and challenges of intense multidisciplinary geothermal exploration activities, 8 years down the road. *Proceedings World Geothermal Congress 2020, Reykjavik, Iceland, April 26 – May 2, 2020.* 12 pp

Moscariello A., Do Couto, D., Omodeo Salé, S.: UNCONGAS Evaluation of unconventional resource potential in the Swiss Plateau: an integrated subsurface study. Département fédéral de l'environnement, des transports, de l'énergie et de la communication DETEC Office fédéral de l'énergie OFEN Recherche énergétique, (2019b), in press.

Moscariello, A. and Geo-Energy Group 2018. Geothermal Exploration in Switzerland for Heat Production and Storage: The Key Role in Knowledge and Technology Transfer From the Hydrocarbon Industry. *Abstract: ACE 2018 Annual Convention & Exhibition, Salt Lake City, (2018).*

Moscariello, A., Clerc, N., Eruteya, O. E., Omodeo-Salé, S. and Guglielmetti, L.: Complex shortening tectonic style in the undisturbed Alpine foreland: Example from the Geneva Basin (Switzerland) and implications for subsurface geo-fluid circulation. *GE-RGBA Report, University of Geneva, GEG2019001 (2019a), 18 pp.*

Moscariello, A., Schneider, A.M. and Filippi, M.L., 1998. Late glacial and early Holocene palaeoenvironmental changes in Geneva Bay (lake Geneva, Switzerland). *Palaeogeography, Palaeoclimatology, Palaeoecology*, 140(1-4), (1998), 51-73.

Moscariello, A.: Quaternary geology of the Geneva bay (Lake Geneva, Switzerland): sedimentary record, palaeoenvironmental and palaeoclimatic reconstruction since the last glacial cycle. *Terre & Environnement*, 4, (1996), xii + 230 pp.

Muralt R., 1999. Processus hydrogéologiques et hydrochimiques dans les circulations profondes des calcaires du Malm de l'arc jurassien (zones de Delémont, Yverdon-les-Bains, Moiry, Genève et Aix-les-Bains). *Matériaux pour la Géologie de la Suisse, série Géotechnique*, 82, 236 pp.

Okasha, T.M., Menouar, H.K., Abu-Khamsin, S.A., and Others, 1998. Oil recovery from tarmat

reservoirs using hot water and solvent flooding. *Journal of Canadian Petroleum Technology*, 37 (04).

Possemiers, M., Huysmans, M. and Batelaan, O., 2015. Application of multiple-point geostatistics to simulate the effect of small-scale aquifer heterogeneity on the efficiency of aquifer thermal energy storage. *Hydrogeology journal*, 23(5), pp.971-981.

Prats, M., 1986. *Thermal Recovery*, volume 7 of SPE Monograph Series.

Røe P, Georgsen F, Abrahamsen P. An Uncertainty Model for Fault Shape and Location. *Math. Geosci.* 2014 Nov 1;46(8):957–69.

Rusillon, E. Characterisation and rock typing of deep geothermal reservoirs in the Greater Geneva Basin (Switzerland & France). *Terre & Environnement* 141 (2018), 252 pp.

Rusillon, E., Chablais, J.: Evaluation des calcaires du Crétacé des forages du LEP : caractérisation de la ressource et préparation au contrôle lithostratigraphique des futurs forages d'exploration GEothermie 2020 (No. Etape 8 : Mesures Porosité-Perméabilité-Densité), Programme GEothermie 2020. Services Industriels de Genève (SIG), Genève. (2017), 15 pp.

Salim, A., Lagraba, P. and Oscar, J., 2018, September. Utilizing Drill Cuttings to Enhance Characterization and Description of Tight Carbonate Reservoirs. In *SPE Annual Technical Conference and Exhibition*. Society of Petroleum Engineers.

Schegg R, Cornford C, Leu W. Migration and accumulation of hydrocarbons in the Swiss Molasse Basin: implications of a 2D basin modeling study. *Mar. Pet. Geol.* 1999 Oct 1;16(6):511–31.

Schegg, R., Cornford, C., and Leu, W., 1999. Migration and accumulation of hydrocarbons in the Swiss Molasse Basin: implications of a 2D basin modeling study. *Marine and Petroleum Geology*, 16 (6), 511–531.

Schweizer D, Blum P, Butscher C. Uncertainty assessment in 3-D geological models of increasing complexity. *Solid Earth*. Copernicus GmbH; 2017 Apr 13;8(2):515–30.

Schweizer, D., Blum, P., and Butscher, C., 2017. Uncertainty assessment in 3-D geological models of increasing complexity. *Solid Earth*, 8 (2), 515–530.

Signer, C. and Gorin, G. E. (1995) 'New geological observations between the Jura and the Alps in the Geneva area, as derived from reflection seismic data', *Ecolgae Geologicae Helvetiae*, 88, pp. 235–265.

Siler DL, Faulds JE, Hinz NH, Dering GM, Edwards JH, Mayhew B. Three-dimensional geologic mapping to assess geothermal potential: examples from Nevada and Oregon. *Geothermal Energy*. SpringerOpen; 2019 Jan 29;7(1):2.

Siler, D.L., Faulds, J.E., Hinz, N.H., Dering, G.M., Edwards, J.H., and Mayhew, B., 2019. Three-dimensional geologic mapping to assess geothermal potential: examples from Nevada and Oregon. *Geothermal Energy*, 7 (1), 2.

Tacher, L., Pomian-Szednicki, I., and Parriaux, A., 2006. Geological uncertainties associated with 3-D subsurface models. *Computers & geosciences*, 32 (2), 212–221.

Eruteya, Guglielmetti, Moscariello, 2021 GR-RGBA 2021003

Thore, P., Shtuka, A., Lecour, M., Ait-Ettajer, T., and Cognot, R., 2002. Structural uncertainties: Determination, management, and applications. *Geophysics*, 67 (3), 840–852.

Trümpy, R., 1980. *Geology of Switzerland: An outline of the geology of Switzerland*. Interbook.

Yielding G., Michie1 E., Bretan P.,Fisher Q 2016. Workflows for Fault Seal Prediction in Siliciclastics and Carbonates Search and Discovery Article #41821 (2016).